



# PET Imaging in Animal Models of Alzheimer's Disease

Baosheng Chen, Bernadette Marquez-Nostra, Erika Belitzky, Takuya Toyonaga, Jie Tong, Yiyun Huang and Zhengxin Cai\*

PET Center, Radiology, Yale School of Medicine, New Haven, CT, United States

## OPEN ACCESS

### Edited by:

Ruiqing Ni,  
ETH Zürich, Switzerland

### Reviewed by:

Nicolas Tournier,  
Commissariat à l'Energie Atomique et  
aux Energies Alternatives (CEA),  
France

Steven Liang,  
Massachusetts General Hospital  
and Harvard Medical School,  
United States

### \*Correspondence:

Zhengxin Cai  
Jason.cai@yale.edu

### Specialty section:

This article was submitted to  
Neurodegeneration,  
a section of the journal  
Frontiers in Neuroscience

Received: 09 February 2022

Accepted: 25 April 2022

Published: 24 May 2022

### Citation:

Chen B, Marquez-Nostra B,  
Belitzky E, Toyonaga T, Tong J,  
Huang Y and Cai Z (2022) PET  
Imaging in Animal Models  
of Alzheimer's Disease.  
Front. Neurosci. 16:872509.  
doi: 10.3389/fnins.2022.872509

The successful development and translation of PET imaging agents targeting  $\beta$ -amyloid plaques and hyperphosphorylated tau tangles have allowed for *in vivo* detection of these hallmarks of Alzheimer's disease (AD) antemortem. Amyloid and tau PET have been incorporated into the A/T/N scheme for AD characterization and have become an integral part of ongoing clinical trials to screen patients for enrollment, prove drug action mechanisms, and monitor therapeutic effects. Meanwhile, preclinical PET imaging in animal models of AD can provide supportive information for mechanistic studies. With the recent advancement of gene editing technologies and AD animal model development, preclinical PET imaging in AD models will further facilitate our understanding of AD pathogenesis/progression and the development of novel treatments. In this study, we review the current state-of-the-art in preclinical PET imaging using animal models of AD and suggest future research directions.

**Keywords:** positron emission tomography, Alzheimer's disease,  $\beta$ -amyloid (A $\beta$ ), tau, neurodegeneration, SV2A, neuroinflammation, animal model

## INTRODUCTION

Dementia is a category of neurodegenerative diseases that mainly affect the daily lives of older people and is characterized by progressive loss of memory, communication, problem-solving/thinking, and motorsensory abilities. The common types of dementia include vascular dementia, frontotemporal dementia, dementia with Lewy bodies, and Alzheimer's disease (AD), which is the most common type and accounts for 60–80% of overall dementia cases (Alzheimer's Association, 2021). Globally, there are 350,000 new cases of early onset dementia per year, and by 2050, 107 million people are predicted to be living with AD, among which 68% reside in the low- and middle-income countries (Global Burden of Disease Study).

The pathological hallmarks of AD are  $\beta$ -amyloid (A $\beta$ )-containing extracellular plaques and oligomers and tau-containing intracellular neurofibrillary tangles (NFTs). The plaques and oligomers interfere with neuron-to-neuron communication at synapses, leading to neurodegeneration. Tau tangles block the transport of nutrients and other molecules inside the neurons, which contributes to neural death. In addition, the A $\beta$  plaque and tau proteins can activate the microglia, which clears these toxic proteins and dead cells but may result in chronic inflammation (Long and Holtzman, 2019). Atrophy, a decrease in brain volume owing to the loss of synapses, dendrites, and neuronal cell bodies, is another biomarker for AD progression (Pini et al., 2016; Halliday, 2017). In addition, the decrease in glucose metabolism further compromises the brain's function (Wang et al., 2016). Familial early-onset AD (FAD) is associated with mutated

genes such as APP, PSEN1, PSEN2, and MAPT, which also significantly increase the risk for late-onset AD (LOAD) (Ryan and Rossor, 2010), while apolipoprotein E variant  $\epsilon 4$  (APOE $\epsilon 4$ ) (Kim et al., 2009) and triggering receptor expressed on myeloid cells 2 (TREM2) are associated with the highest risk of developing LOAD (Wolfe et al., 2018). These dominantly inherited Alzheimer's disease (DIAD) caused by rare genetic mutations are associated with increased levels of A $\beta$  and tau, decreased glucose metabolism, and brain atrophy 10–20 years before the symptoms set in. In addition, multiple enzymes are associated with AD, including the  $\beta$ -site APP cleaving enzyme 1 (BACE1) (Das and Yan, 2017), caspase 3 (Rohn, 2010), and aspartyl cathepsin (Haque et al., 2008), among others.

Animal models of AD have become essential for studying the pathogenesis and progression of AD pathology and for validating the mechanism of action of novel therapeutics before translation to human trials (Alzheimer's Association, 2021). Many animal models have been developed to mimic the pathophysiological processes and progression mechanisms of AD and to preclinically test treatment methods (Figure 1). Both invertebrate and vertebrate animals have been used in modeling the aging and certain aspects of AD processes, as genetically modified animals that recapitulate certain traits of AD are needed to understand the pathological and biological mechanisms of AD. Because there has not been a rodent model that completely recapitulates human AD, rodent models have been mainly used for proving mechanisms of action for therapeutic interventions or testing the target binding specificity of imaging probes. A fully characterized AD animal model with stable phenotypes and a clear disease onset time can greatly help address the specific scientific questions.

Many neuroimaging methods, such as magnetic resonance imaging (MRI; structural and functional), computerized tomography (CT), and positron emission tomography (PET), have been increasingly employed to evaluate AD neurodegeneration. PET imaging uses radiolabeled tracers to detect and quantify cerebral and metabolic changes by targeting specific biomarkers that are associated with AD. Fluorodeoxyglucose (FDG) PET detects brain metabolism and amyloid PET that quantifies the amyloid deposit has been developed to understand AD pathogenesis and to monitor disease progression and therapeutic effects. Other neuro-specific, inflammation- and metabolic-associated radiotracers are under development for AD studies. In this study, we discuss the AD animal models that are relevant in AD PET imaging studies and summarize the PET tracers that have been tested in AD animal models and the findings from these studies.

## AD ANIMAL MODELS

### Mouse Models

In the field of neurodegenerative diseases, mice are the most commonly used animals for their biological features that are similar to those of humans, easily manipulated genetics to mimic human conditions and diseases, and a relatively short life span (1.5–2 years). Because mice do not develop AD

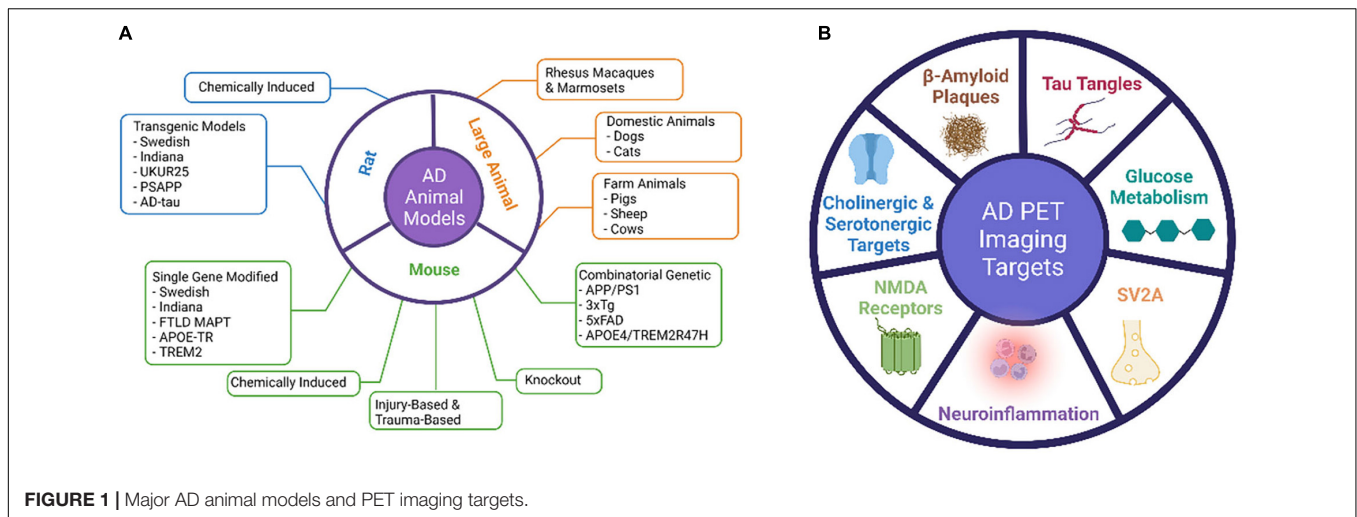
naturally, transgenic mice are generated to recapitulate certain AD pathological features to fit the research needs (Table 1). The genes associated with the early onset of AD have been the main targets for transgenic manipulations.

### Mice With the Familial APP Mutations V717F (Indiana) and K670N/671L (APP<sup>swe</sup>, Swedish)

The first A $\beta$  plaque-developing mouse model is APP (V717F), which progressively develops extracellular thioflavin S-positive A $\beta$  deposits, neuritic plaques, synaptic loss, astrocytosis, and microgliosis (Games et al., 1995). This model can be used for testing therapeutic drugs targeting amyloidosis. The commonly studied Swedish APP mutation (APP<sup>swe</sup>) K670N/M671L carries a transgene coding for the 695-amino acid isoform of human A $\beta$  precursor protein bearing the Swedish mutation (Sturchler-Pierrat et al., 1997). This mouse model expresses high concentrations of the mutant A $\beta$ , develops significant amyloid plaques, and displays memory deficits. It is useful for studying APP expression, amyloid plaque formation, neuronal decline, and memory loss associated with AD, as well as drug discoveries. Recently, Xu et al. (2015) achieved the amyloid deposition using murine genes carrying the APP<sup>swe</sup> mutation, indicating murine A $\beta$  peptides can produce amyloid deposits that morphologically resemble those found in human AD.

### Mice With the Familial FTL D MAPT Mutation P301L or Human Tau

The first NFT-developing mouse was achieved by expressing the familial FTL D MAPT mutation P301L under the control of the mouse prion promoter (Lewis et al., 2000). Allen et al. (2002) used mouse Thy1.2 promoter to reach a 2-fold increase in the expression of P301S mutant FTL D-tau compared with endogenous tau, with NFTs forming at 5 months of age. The first human MAPT transgenic model (ALZ7) with the human THY1.2 promoter expressed only a low level of the transgenic gene but achieved deposition of hyperphosphorylated tau in the somatodendritic domain (Gotz et al., 1995). The rTg4510 model uses a reversible binary transactivator system to achieve a high level of tau expression (13-fold) with P301L, NFT-like lesions, neuronal loss, cognitive impairment, and brain atrophy at an earlier time frame (Santacruz et al., 2005). This mouse develops progressive intracellular tau aggregations in the corticolimbic areas and forebrain atrophy. The human Tau (hTau) mice (Andorfer et al., 2003) were generated by crossing 8c mice expressing human 3R and 4R tau isoforms (Duff et al., 2000) with tau knockout (KO) mice generated by targeted disruption of exon one on the MAPT gene (Tucker et al., 2001). This mouse model expresses all six isoforms of hTau but lacks mouse tau. It develops age-associated tau pathology that appears most severe in the neocortex and hippocampus. No tau pathology was found in both 8c mice and tau KO mice. Recently, Saito et al. (2019) used a homologous recombination approach to replace the entire murine *Mapt* gene with the human ortholog to create a *MAPT* knock-in (KI) mouse model that expresses all six tau isoforms present in humans. They cross-bred the *MAPT* KI mice with single *App* KI mice to generate the APP/MAPT double knock-in



(dKI) mice that exhibit higher tau phosphorylation than the single MAPT KI mice (Saito et al., 2019).

### APOE-Target Replacement Mice (APOE-TR Mice)

The APOE family consists of three isoforms: APOE2, APOE3, and APOE4, with APOE4 being the greatest genetic risk factor for AD (Kim et al., 2009). APOE-target replacement mice (APOE-TR Mice), in which the m-APOE coding sequence is replaced by that of an h-APOE allele, display alterations in synaptic number and structure, network connectivity, and behavior based on the specific APOE isoform expressed (Ji et al., 2003; Wang et al., 2005; Tai et al., 2011; Zhu et al., 2012; Dumanis et al., 2013; Koutseff et al., 2014; Neustadt et al., 2017; Lewandowski et al., 2020). These mice exhibit isoform-specific differences in lipid physiology and synaptic function. Mice with h-APOE4 exhibit earlier and more severe AD pathology and memory decline (Bour et al., 2008; Sun et al., 2017; Lewandowski et al., 2020).

### Triggering Receptor Expressed on Myeloid Cells 2 Gene-Modified Mice

Triggering receptor expressed on myeloid cells 2 (TREM2) is expressed in microglia, and its genetic variants R47H and Y38C are linked to AD, frontotemporal dementia, and Nasu-Hakola disease, which is an early onset of dementia characterized by white matter pathology (Yaghmoor et al., 2014). While Trem2 variant R47H is largely associated with late-onset AD, Trem2 variant Y38C is associated with the development of early onset dementia (Jadhav et al., 2020). Both Trem2R47H and Trem2Y38C mice were generated using the CRISPR/Cas9 technique to introduce the point mutations of Trem2R47H and Trem2Y38C. TREM2 R47H homozygous mice exhibit a novel splice variant resulting in partial expression of mRNA and protein in the brain (Xiang et al., 2018). While mice harboring the Trem2 Y38C exhibited normal expression levels of TREM2, alterations were observed in the expression of neuronal and oligodendrocyte/myelin genes, along with regional decreases in synaptic protein levels, particularly in the hippocampus (Jadhav et al., 2020).

### APP/PS1 Mice

In addition to the “single-gene models” described above, combinations of AD-related genes have also been introduced in mice using transgenic technology. These combinatorial genetic models present greater phenotypical diversity, and thus offer more options for preclinical studies. The APP/PS1 mouse model was generated by administration of both APP<sup>swe</sup> mutant (K595N/M596L) and the  $\Delta$ E9 mutant of presenilin 1 (PS1), which is an essential component of  $\gamma$ -secretase, the enzyme responsible for APP cleavage. Mutations in PS1 lead to dominant inheritance of early-onset FAD (Jankowsky et al., 2001). The mice develop A $\beta$  deposits in the brain by 6–7 months of age, with 15-month-old females presenting a 5-fold (A $\beta$ 42) and 10-fold (A $\beta$ 40) increase in A $\beta$  deposits in the cerebellum compared to males (Jankowsky et al., 2004; Ordonez-Gutierrez et al., 2016).

### The 3 $\times$ Tg Strain

Although there are no reports that APP, PS1, and tau mutations occurring simultaneously in humans, the 3  $\times$  Tg strain is the most widely used model that presents aggregated A $\beta$  and synaptic dysfunction. This model is created by co-injecting two constructs expressing APP<sup>swe</sup> and P301L mutant tau into oocytes obtained from PS1 M146V KI mice. These triple transgenic mice express mutant APP, PSEN2, and MAPT and show age-dependent accumulation of A $\beta$  plaques and neurofibrillary tangle-like pathology, starting around 4 months of age (Grueninger et al., 2010).

### The 5 $\times$ FAD Strain

The 5  $\times$  FAD strain combines the APP<sup>swe</sup> mutation with the Florida (I716V) and London (V717I) mutations of APP, as well as the M146L and L286V mutations of PSEN1. These mice show progressive cognitive deficits with several pathological hallmarks of AD, such as A $\beta$  plaques, gliosis, synaptic degeneration, and neuronal loss, and develop tau pathology (Oakley et al., 2006).

### The APOE4/TREM2R47H Mouse

This double mutant strain carries a humanized APOE4 knock-in mutation and a CRISPR/cas9-generated R47H point mutation

**TABLE 1** | List of major AD mice models.

#	Strain name	Genetic modification	Genetic background	Age of AD pathology first appear (month)	AD related pathology
1	Tg2576 (APPSwe)	APP KM 670/671NL	B6; SJL	5 m	Extensive amyloid pathology
2	JNPL3(P301L)/Tg(Prnp-MAPT*P301L)	htau with P301L mutation	B6, DBA/2, SW	4.5 m/homo. and 6.5 m/hemi.	Homozygous develops human-like tauopathies faster than the hemizygous model
3	APP/PS1	Chimeric Mo/HuAPP695swe and a mutant hPS1 (PS1-dE9)	B6;C3	6 m	Early-onset of amyloid plaque
4	ARTE10 (APP-PS1)16347	hAPP 695-a.a. isoform with Swedish mutation and hPS1 with M146V mutation	B6	3 m/homo. and 5 m/hemi.	Robust and reliable plaque pathology
5	APPSWE-TAU-2469	hAPP695-a.a. isoform and hMAPT P301L mutation	B6, DBA/2, SJL, SW	3 m	similar plaque pathology to Tg2576 with more extensive neurofibrillary tangles than the JNPL3.
6	3xTg-AD	APP KM 670/671NL, MAPT P301L, and PS1 M146V	B6;129	6 m	age-related and progressive plaques and tangles. tau pathology at 12 m. Synaptic dysfunction occur before plaques and tangles
7	5xFAD, TG6799	hAPP695 isoform with Swedish KM 670/671NL, Florida (I716V), London (V717I), hPS1 with M146L and L286V mutations	B6, B6SJLF1	2 m	Amyloid pathology; reduced synaptic marker protein levels
8	APOE3	hAPOE3 from the endogenous APOE locus	B6	NA	NA
9	APOE4	hAPOE4 allele from the endogenous APOE locus	B6	4 m	Decreased levels of total cholesterol, LDL and HDL
10	Trem2*R47H	an R47H point mutation and two silent mutations (lysine AAG > AAA and alanine GCC > GCA) into mTrem2	B6	NA	NA
11	Trem2*Y38C	Y38C point mutation	B6	NA	TREM2-deficient microglia fail to proliferate and cluster around plaques
12	APOE4/Trem2*R47H	hAPOE4 knock-in mutation and R47H point mutation	B6	NA	NA
13	HApp/APOE4/Trem2*R47H	triple mutants with hAPOE4, R47H mutation mTrem2, and a hAPP within the mApp	B6	NA	the human A $\beta$ generated by these mice is more aggregation-prone than the endogenous mouse A $\beta$

of the Trem2 gene. This strain does not produce any severe phenotypes, even late in life, allowing a better understanding of the effect of AD risk factors in the context of aging (Kotredes et al., 2021).

### Knockout Mice

Several AD-related KO mice are generated for understanding the pathophysiological role of AD-related proteins, including APP, MAPT, BACE1, APOE, PSEN1, PSEN2, and Trem E (Table 2).

APP KO mice display deficits in forelimb grip strength and locomotor activity and an age-related deficit in retention of memory for an aversive experience (Senechal et al., 2008). MAPT KO mice have been reported to show less evidence of brain dysfunction (Harada et al., 1994; Dawson et al., 2001; Morris et al., 2011). PSEN1 KO mice exhibit perinatal lethality in homozygous animals, which die shortly after birth (Shen et al., 1997). PSEN2 KO mice are viable and normal in growth and size and do not display any gross brain abnormalities,

astrogliosis, or behavioral abnormalities by 12 months of age, and no deficit in APP processing (Herreman et al., 1999). APOE KO mice display poor lipoprotein clearance with subsequent accumulation of cholesterol-ester-enriched particles in the blood (Piedrahita et al., 1992). The systemic proinflammatory status of APOE KO mice also makes them good candidates for studying risk factors for AD (Lo Sasso et al., 2016). TREM KO mice show no behavioral and cognitive deficit (Kang et al., 2018). BACE1 KO mice do not display any gross physical or behavioral abnormalities (Cai et al., 2001).

### Chemical-Induced AD Models

Alzheimer's disease models can also be generated by chemical induction. Synthetic A $\beta$  and tau aggregates have been intraperitoneally injected to induce cerebral amyloids and intracerebral tauopathy (Gotz et al., 2001; Clavaguera et al., 2014). Intracranial injection of okadaic acid, a protein phosphatase inhibitor, increased tau phosphorylation and

**TABLE 2** | List of AD-related gene knockout mice models.

#	Strain name	Genetic modification	Genetic background	Phenotype
1	APP <sup>-/-</sup>	APP gene was disrupted by inserting a stop codon into the first exon through homologous recombination	B6	Deficits in forelimb grip strength and locomotor activity and an age-related deficit in retention of memory for an aversive experience (Senechal et al., 2008)
2	PS1	Psen1 knock-out	B6	A drastic reduction in neural progenitor cells in the embryo with death occurring minutes after being born
3	MAPT <sup>-/-</sup>	A PGK-neo cassette is inserted into the first exon of tau, only short fragments incapable of binding to MTs	129 × B6	Not much evidence of brain dysfunction (Dawson et al., 2001)
4	PSEN1 <sup>-/-</sup>	Disruption of exons 1 to 3	129 × B6	Perinatal lethal in homozygous animals which die shortly after birth (Shen et al., 1997)
5	PSEN2 <sup>-/-</sup>	The replacement of exon 5 by the hygromycin cassette results in a frame shift between exons 4 and 6.	129 × B6	Do not display any gross brain abnormalities, astrogliosis, or behavioral abnormalities by 12 m. APP processing is not affected (Herreman et al., 1999)
6	APOE2-1547	Homozygous for a human APOE2 gene targeted replacement of the endogenous mouse APOE gene	129 × B6	Hyperlipoproteinemia with elevated plasma cholesterol and triglyceride levels, decreased clearance of vLDL particles, and spontaneous atherosclerotic plaques on a normal diet, exacerbated by a high fat diet
7	APOE3 1548	Homozygous for a human APOE3 gene targeted replacement of the endogenous mouse APOE gene	129 × B6	Increased risk of atherosclerosis and hypercholesterolemia compared with wild type mice on a high fat diet, but not on a normal diet
8	APOE4-1549	Homozygous for a human APOE4 gene targeted replacement of the endogenous mouse APOE gene	129 × B6	At increased risk of atherosclerosis compared with wild-type animals or mice expressing human APOE3
9	Trem2 KO (KOMP)	The entire coding region of the Trem2 gene was replaced by Velocigene cassette ZEN-Ub1 (lacZ -p(A)-loxP-hUbCpro-neor-p(A)-loxP)	B6	Trem2 <sup>-/-</sup> microglia show less proliferative activity and less pronounced changes in morphology than do wild-type microglia after an excitotoxic insult no behavioral and cognitive deficit (Kang et al., 2018)
10	BACE1 <sup>-/-</sup>	Targeted deletion in the mouse gene $\beta$ -site APP cleaving enzyme 1	129 × B6	Do not display any gross physical or behavioral abnormalities (Cai et al., 2001)

protein aggregation in distinct brain regions (Baker and Gotz, 2016). Intracranial injection of synthetic A $\beta$  aggregates into P301L tau transgenic mice can accelerate NFT formation (Peeraer et al., 2015). Brain lysates from both transgenic mice and patients with AD also induce nucleation of protein aggregation along with neuronal projections in healthy mice or mice with preexisting AD pathology (Bolmont et al., 2007; Clavaguera et al., 2009; He et al., 2018). Lipopolysaccharide (LPS) acts as a Toll-like receptor 4 ligand to activate microglia to produce proinflammatory cytokines such as TNF- $\alpha$ , IL-1 $\beta$ , prostaglandin E<sub>2</sub> (PGE<sub>2</sub>), and nitric oxide (NO) in the central nervous system (Heneka et al., 2015). The administration of LPS to animals induces cognitive impairment (Shaw et al., 2001; Choi et al., 2012) and high levels of A $\beta$ <sub>1-42</sub> (Zhao et al., 2019).

Other chemicals used for the induction of cognitive impairment include heavy metals (e.g., aluminum, cobalt, and copper), scopolamine, ethanol, colchicine, an excitotoxin, streptozotocin, and sodium azide, among others, and have been nicely summarized in the review (More et al., 2016; Götz et al., 2018).

### Injury-Based and Trauma-Based Models

Brain injury is associated with elevated A $\beta$  levels and tau phosphorylation (Yu et al., 2012), but not the formation of plaques and NFTs. In transgenic hTau and 3xTg mice, brain

injury accentuates the development of tau pathology and A $\beta$  accumulation (Tran et al., 2011; Ojo et al., 2013).

### Next-Generation AD Models

There is no AD mouse model that recapitulates all aspects of human AD. Even with the high levels of amyloid protein, the mice still do not display human-like cognitive deficits. The A $\beta$  plaques in mice are often diffuse or exhibit fewer crosslinking fibrils even when they appear condensed. The tau pathology also shows a certain difference from humans, with a wide and uncontrollable range of expression levels in some AD model mice. Because there are dozens of different genes that are associated with AD, the different combinations of mutations in these genes, in conjunction with varying environmental stimulators, will contribute to each unique AD case (Naj and Schellenberg, 2017). Furthermore, the offspring of AD transgenic and wild mice are more likely to develop memory loss, indicating there are AD-associated genetics or environmental factors yet to be elucidated, which drives the continuing efforts for better mouse models. In 2016, the NIH started the MODEL-AD consortium to engineer mice with different genetic mutations associated with early- or late-onset AD (model-ad.org).

### Rat Models

Compared to mice, rats are easier to handle and have larger brain sizes for easier surgical operation and imaging

**TABLE 3** | List of major AD rat models.

#	Strain name	Genetic modification	Genetic background	Age of AD pathology first appear (month)	AD related pathology
1	TgAPP <sup>swe</sup>	hAPP KM 670/671NL	Fischer-344	NA	No extracellular A $\beta$ deposits
2	Tg6590	hAPP KM 670/671NL	Sprague-Dawley	11 m	The levels of both A $\beta$ species are increased 65% in hippocampus and 40% in cortex of 11-month-old animals.
3	McGill-R-Thy1-APP	hAPP751 with K670N/671L and V717F	HsdBrl:WH Wistar	6–9 m	Homozygotes show age-dependent accumulation of A $\beta$ plaques, gliosis, cholinergic synapse loss. Intracellular A $\beta$ inclusions appears at postnatal day 7 and A $\beta$ plaques at around 6–9 m
4	Tg1116	hAPP minigene containing K670N/671L and V717F	Sprague-Dawley	NA	NA
5	APP21	hAPP double mutant construct containing K670N/671L and V717F	Fischer-344	NA	NA
6	APP31	hAPP double mutant construct containing the K670N/671L and V717F	Fischer-344	NA	NA
7	Tg478/Tg1116	hAPP with K670N/671L and V717F	Sprague-Dawley	17–18 m	A $\beta$ for amyloid deposition
8	TgF344-AD	APP <sup>swe</sup> and PS1 $\Delta$ E9	Fischer-344	6 m	Age-dependent accumulation of A $\beta$ plaques in hippocampus and cortex with age-dependent cerebral amyloidosis that precedes tauopathy, gliosis, apoptotic loss of neurons in the cerebral cortex and hippocampus and cognitive dysfunction. Tau pathology is reported
9	UKUR25	hAPP with K670N/671L and V717F and PS1 (M146L)	Wistar	NA	Intracellular accumulation of A $\beta$ in hippocampus and cortex without extracellular amyloid
10	PS/APP (Tg478/Tg1116/Tg11587)	hAPP695 with K670N/671L and V717F and PSEN1 with $\Delta$ E9 (4.6 kb deletion of exon 9)	Sprague-Dawley	7 M	A $\beta$ deposition
11	SHR24	Human non-mutated truncated tau encompassing 3R domains and a proline-rich region (3R tau151–391)	SHR	9 m	Age-dependent progressive neurofibrillary degeneration in the isocortex

analysis (Ellenbroek and Youn, 2016). Both genetic and non-genetic rat AD models have been developed (Table 3). However, unlike transgenic AD mouse models, not as many AD rat models are available for scientific research and rats appear to be more resilient to AD pathology than mice (Charreau et al., 1996).

### Rat Models With the Familial Swedish and Indiana Mutations

The APP transgenic rats appear to have lower expression levels of the APP transgene than the mouse AD model (Benedikz et al., 2009). TgAPP<sup>swe</sup> is the first APP transgenic rat that overexpresses human APP with Swedish mutation (K670N and M671L) (Ruiz-Opazo et al., 2004), with only a 56.8% increase in the expression level of APP mRNA, 21% increase for A $\beta$ <sub>42</sub>, and 6% for A $\beta$ <sub>40</sub> in the brain. No AD-related pathology was found in these animals up to the age of 18 months. The Tg6590 rat generated by Fokesson et al. is another model that carries

human APP with the Swedish mutation. The levels of both A $\beta$  species are increased by 65% in the hippocampus and 40% in the cortex of 11-month-old animals. The rats display learning and memory deficits in the Morris water maze at 9 months and altered spontaneous behavior measured in open field (Kloskowska et al., 2010). The McGill-R-Thy1-APP rat model expressed hAPP751 bearing the Swedish and Indiana mutations, with intracellular A $\beta$  inclusions detected as early as postnatal day 7 and A $\beta$  plaques at 6–9 months of age (Leon et al., 2010). The Tg1116 rats express a human APP minigene containing both the Swedish and Indiana familial AD mutations (Flood et al., 2009). APP21 and APP31 express a human APP double mutant construct containing the Swedish and Indiana AD mutations driven by the ubiquitin-C promoter. The APP transgene is reported to be expressed in the brain, in neuronal but not glial cells (Agca et al., 2008). No pathological or behavioral studies have been published yet. The double homozygous Tg478/Tg1116 rats were generated by crossing Tg478 which expresses human APP with the Swedish

mutation (Flood et al., 2009) and Tg1116. The rats produce sufficient levels of A $\beta$  for amyloid deposition to occur by the age of 17–18 months (Flood et al., 2009).

### APP<sub>swe</sub> and PS1 $\Delta$ E9/TgF344-AD Rats

TgF344-AD rats co-express APP<sub>swe</sub> and PS1 $\Delta$ E9 transgenes and present with age-dependent cerebral amyloidosis that precedes tauopathy, gliosis, apoptotic loss of neurons in the cerebral cortex and hippocampus, and cognitive dysfunction (Cohen et al., 2013).

### Rat Model With the Familial APP Mutations V717F (Indiana) and Swedish APP (APP<sub>swe</sub>) K670N/671L and Human PSEN1 With the Finnish M146L Mutation

UKUR25 rats express human APP containing the Swedish and Indiana (V717F) mutations, and mutated PS1 (M146L). The main pathological feature was an intracellular accumulation of A $\beta$  in neurons of the hippocampus and cortex without extracellular amyloid up to 24 months of age. Mild impairment in acquisition learning was found in 16-month-old male rats, with an increase in tau phosphorylation at S396 and S404 ERK2 sites (Echeverria et al., 2004a,b).

### PSAPP (Tg478/Tg1116/Tg11587) Rats

The PSAPP model rats express hAPP695 carrying the Swedish and London (K670N/M671L and V717I, respectively) mutations together with PSEN1 carrying the Finnish mutation (PS1,  $\Delta$ E9) and develop A $\beta$  deposition around 7 months of age (Flood et al., 2009). This strain was created by crossing double homozygous Tg478/Tg1116 rats with Tg11587 that carries a human PS-1 transgene with the familial AD mutation M146V. The homozygous rats produce sufficient levels of A $\beta$  for amyloid deposition to occur by the age of 7 months. The triple homozygous transgenic rat, Tg478/Tg1116/Tg11587, has also been called the PSAPP rat. The compact amyloid deposits were found to be associated with activated microglia, reactive astrocytes, and phosphorylated tau immunoreactivity.

### AD-Tau Rat Model

Overexpression of human non-mutated truncated tau encompassing 3R domains led to the first rat model of progressive cortical neurofibrillary degeneration (Filipcik et al., 2012). This transgenic rat expresses a truncated form of the human tau protein (truncated at amino acid positions 151–391), which is found in the brains of sporadic AD patients (Benedikz et al., 2009).

### Chemical-Induced AD Rat Models

The aforementioned chemicals used to generate AD mouse models can also be employed in rats to create AD phenotypes (More et al., 2016; Götz et al., 2018).

### Large Animal AD Models

Non-human primates such as rhesus macaques and marmosets are not known to develop AD but do accumulate A $\beta$  deposits and show tauopathy in their aged brains (Paspalas et al., 2018; Haque and Levey, 2019; Arnsten et al., 2021b; Datta et al.,

2021; Leslie et al., 2021). Intracranial injection of A $\beta$ <sub>42</sub> and thiorphan, an inhibitor of neprilysin that is responsible for A $\beta$  clearance, has been employed to generate an AD model in middle-aged (16–17 years) rhesus monkeys (Li et al., 2010). Significant intracellular accumulation of A $\beta$  was found in the neurons of the basal ganglia, cortex, and hippocampus, accompanied by neuronal atrophy and loss. Two injections of an adeno-associated virus expressing a double tau mutation (AAV-P301L/S320F) in the left hemisphere of rhesus monkeys result in misfolded tau propagation similar to that in humans. Tau spreading is accompanied by robust neuroinflammatory response driven by TREM2 + microglia, with biomarkers of inflammation and neuronal loss in cerebrospinal fluid and plasma (Beckman et al., 2021).

Other non-primate large animals used for AD modeling include domestic animals such as dogs and cats as well as farm animals including pigs, sheep, and cows. Aged dogs develop plaque pathology and cerebral amyloid angiopathy (Yu et al., 2011), as well as a dementia-like syndrome resembling human AD (Prpar Mihevc and Majdic, 2019; Abey et al., 2021). Tau dysfunction and tangles have been reported and associated with cognitive decline (Yu et al., 2011; Schmidt et al., 2015; Smolek et al., 2016). Cats also develop plaques, tangles, and brain atrophy along with cognitive decline as they age (Chambers et al., 2015; Fiock et al., 2020). Two transgenic pig models of AD have been reported using minipigs. The first one carries an hAPP transgene with the Swedish mutation driven by the human BDGF $\beta$  promoter, resulting in high levels of brain-specific A $\beta$  expression (Kragh et al., 2009), and the second minipig model carries three copies of a transgene expressing the 695 variant of hAPP with the Swedish mutation and a human PSEN1 transgene with the M146L mutation (Jakobsen et al., 2016). Intraneuronal accumulation of A $\beta$ <sub>1–42</sub> was detected in two pigs: one at 10 months and one at 18 months. Plaque- and tangle-like pathologies have also been seen after traumatic brain injury (TBI) in pigs (Hoffe and Holahan, 2019). Tau pathology and A $\beta$  plaques have been identified in aged sheep and goats as well (Braak et al., 1994).

## PRECLINICAL PET IMAGING IN AD ANIMAL MODELS

### $\beta$ -Amyloid Imaging

The development and validation of the first-in-class A $\beta$  PET radiotracer, the thioflavin T-derived Pittsburgh compound B ([<sup>11</sup>C]PIB or PIB), was a milestone in AD imaging. It not only allows the direct *in vivo* visualization and quantification of A $\beta$  plaque in living subjects (Klunk et al., 2004) but also paves the road for the development and FDA approval of its <sup>18</sup>F-labeled analog ([<sup>18</sup>F]flutemetamol), the stilbene derivative [<sup>18</sup>F]florbetaben, and the styrylpyridine derivative [<sup>18</sup>F]florbetapir, the use of which have become impactful in AD clinical trials and diagnosis. The intrinsic fluorescent characteristics of these imaging probes and their analogs allow for the microscopic assessment of their binding selectivity and binding preference to different forms of A $\beta$  plaques

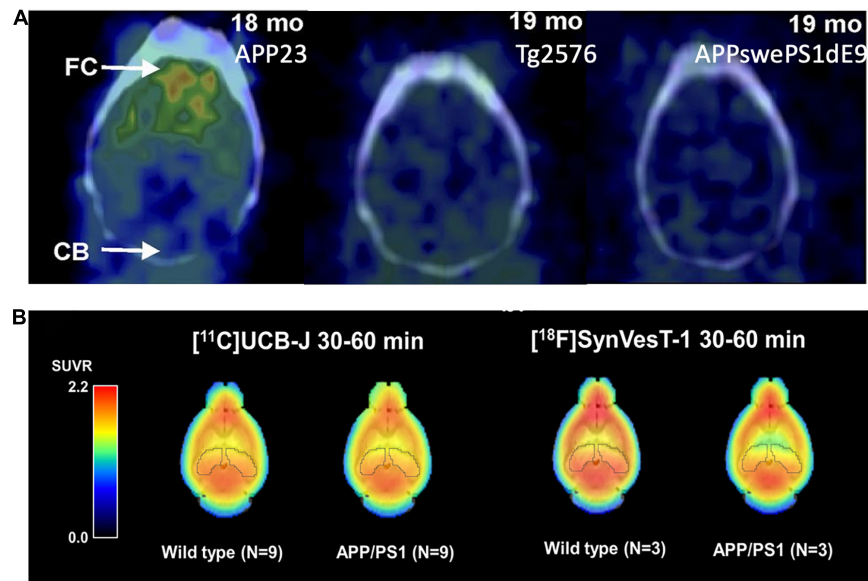


**FIGURE 2 | (A)** [ $^{11}\text{C}$ ]PIB binding to A $\beta$  deposits varies by mouse strains. APP23: Extensive A $\beta$  deposits; Tg2576: Mild A $\beta$  deposits; APP-swePS1dE9: Extensive A $\beta$  deposits. This figure was adapted and modified from Snellman et al. *J Nucl Med.* 2013;54:1434-1441. **(B)** Uptake of the SV2A PET tracers [ $^{11}\text{C}$ ]UCB-J and [ $^{18}\text{F}$ ]SynVesT-1 in the brain of APP/PS1 and wild-type mice. The uptake of both tracers was lower in the hippocampus of APP/PS1 mice compared to wild-type controls.

and A $\beta$  plaques at different locations (e.g., parenchymal and cerebral amyloid angiopathy, CAA) (Bacsikai et al., 2003; Fodero-Tavoletti et al., 2012).

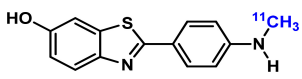
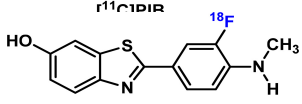
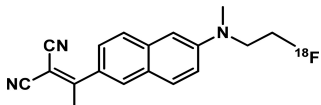
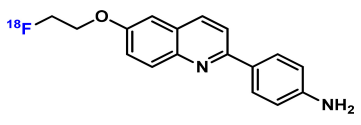
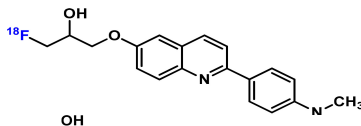
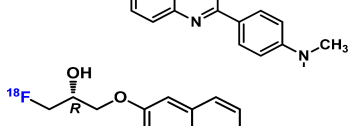
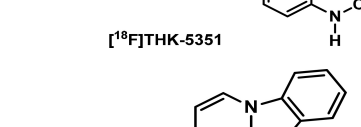
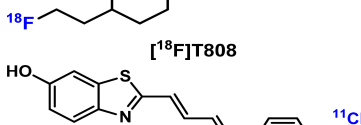
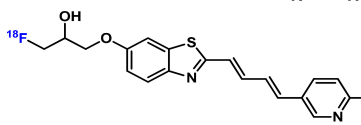
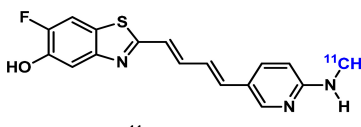
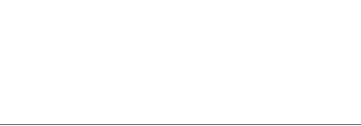
Many A $\beta$  imaging tracers have been evaluated using multiple different AD animal models, mainly in AD mice. PIB has been tested in AD mice of APPswe, APP/PS1, 3  $\times$  Tg, 5  $\times$  FAD, Tg2576, and APP23 (Ni, 2021). Initial reports on PIB binding in Tg2576 and APP/PS1 mice at advanced ages were negative, even with abundant A $\beta$  pathology (Klunk et al., 2005; Toyama et al., 2005); while PIB binding in APP23 mice was positive (Maeda S. et al., 2007). These data led to the hypothesis that the paucity of high-affinity binding sites for PIB in murine A $\beta$  plaques requires very high molar activity PIB for successful imaging in murine AD models. Snellman et al. (2013) compared PIB uptake longitudinally in the brains of multiple AD mouse models and found higher PIB uptake in the cortex of APP23 mice compared with the wild-type controls and no difference in APP/PS1 and Tg2576 mice with their corresponding controls, consistent with previous results from other groups (Figure 2A). They also compared the thioflavin-T staining patterns and found that APP23 mice form large and compact human-like A $\beta$  deposits, whereas Tg2576 mice and APP/PS1 mice form sparse fibrillar deposits. The results suggest that PIB binding is highly dependent on the AD model and the associated higher-order fibrillar structure rather than simple  $\beta$  sheets. At a microscopic level, the A $\beta$  plaques formed in early onset autosomal dominant AD and sporadic AD brains have different levels of non-fibrillar A $\beta$  species (Querol-Vilaseca et al., 2019), and the A $\beta$  deposits in familial AD, sporadic AD, and cerebral amyloid angiopathy manifest different conformations (Condello et al., 2018). Further understanding of the interactions of the imaging

probes with amyloid plaques of different forms will help with the development of probes targeting the various forms of misfolded A $\beta$  proteins in the brain (Biancalana and Koide, 2010).

One of the biggest advantages of small animal PET imaging is the longitudinal tracking of the pathogenesis and therapeutic effects of experimental drugs. This was demonstrated by the longitudinal PET imaging studies in AD animal models (Maeda J. et al., 2007; Deleye et al., 2017; Snellman et al., 2017). The challenges in imaging A $\beta$  plaques in AD animal models are due to the different forms of plaques and disposition patterns in different animal models and at different ages of the same animals (Snellman et al., 2013). Other challenges are the quantification of the PET signals. For the quantitative analysis of human A $\beta$  PET imaging data, the cerebellum was chosen as the reference region to generate distribution volume ratio (DVR) or standardized uptake value ratio (SUVR) because of the lack of specific binding of PIB in the human cerebellum (Lopresti et al., 2005; Price et al., 2005). However, there are emerging effective drugs targeting other pathological pathways and that do not alter A $\beta$  plaque levels, e.g., Fyn inhibitor and mGluR5 silent allosteric modulator (SAM) (Kaufman et al., 2015; Haas et al., 2017). Thus, the objective assessment of their treatment effects needs different imaging biomarkers that are closely related to synaptic/functional recovery rather than A $\beta$  plaque levels. The current consensus considers A $\beta$  oligomers as the primary cause of the neurotoxicity derived from abnormal amyloidosis. Thus, the development of an imaging agent targeting A $\beta$  oligomers is highly desirable, albeit challenging.

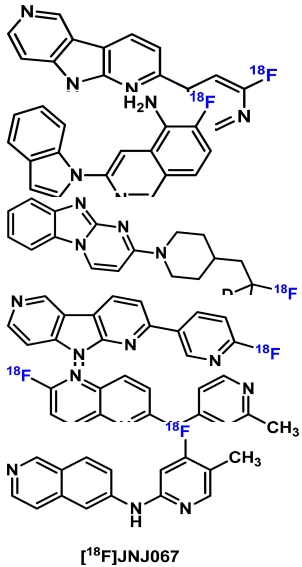
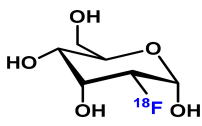
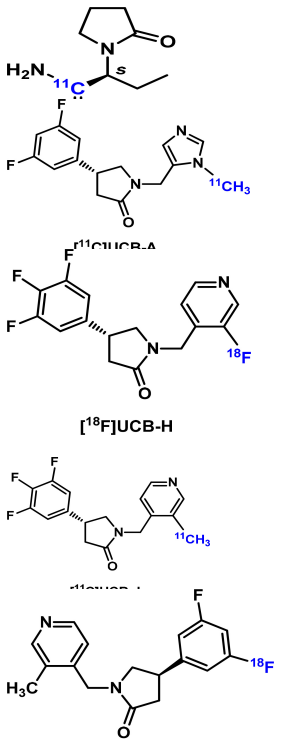
Large molecules such as antibodies have been developed for A $\beta$  PET imaging. Sehlin et al. (2016) and Fang et al. (2019) engineered the  $^{124}\text{I}$ -labeled A $\beta$  antibodies [ $^{124}\text{I}$ ]mAb158

**TABLE 4** | Summary of selected AD tracers.

Imaging target	Tracer structure	Imaging characteristics	Major finding	Reference
$\beta$ -Amyloid	 <b>r<sup>11</sup>C]PIB</b>	High binding affinity to large and compact A $\beta$ deposits	Milestone in AD imaging	Rabinovici et al., 2007
	 <b>[<sup>18</sup>F]Flutemetamol</b>	Similar to PIB but with higher non-specific binding in brain	FDA approved	Zeydan et al., 2021
TAU	 <b>[<sup>18</sup>F]FDNDP</b>	Binds to both amyloid plaques and tau tangles	First PET tracer to visualize both amyloid plaques and tau tangles in living humans. No different uptake was found between Tg2576 and WT litter mates	Tauber et al., 2013
	 <b>[<sup>18</sup>F]THK523</b>	Neurofibrillary tau tangles, off-target binding to MAO-B	First tau selective tracer. Higher retention in rTg4510 and APP/PS1 brains	Fodero-Tavoletti et al., 2011
	 <b>[<sup>18</sup>F]THK5105</b>		[ <sup>18</sup> F]THK-5105 was tested clinically and evaluated in terms of whether it could selectively bind to tau aggregates in living patients with AD	Okamura et al., 2014
	 <b>[<sup>18</sup>F]THK5117</b>		Increased SUVR in subbrain regions in PS19 and biTg mice	Alzghool et al., 2021
	 <b>[<sup>18</sup>F]THK-5351</b>		PET signal correlated well with histo and biochemical tau level in P301S tau mice	Rodriguez-Vieitez et al., 2017
	 <b>[<sup>18</sup>F]T808</b>		The most widely studied first-generation tau radioligand. Increased uptake in PS19 mice. More sensitive than [ <sup>18</sup> F]THK5117 in PS19 strain. No increase in P301L tau mice	Declercq et al., 2016
	 <b>[<sup>11</sup>C]PM-PBB3</b>	tau deposits	Clinically detect tauopathies in human brain. Increased uptake in rTg4510 mice brain both <i>in vivo</i> and <i>in vitro</i>	Chiotis et al., 2018
	 <b>[<sup>11</sup>C]LM229</b>		Increased uptake in 6 month old rTg4510 mice	Su et al., 2020
	 <b>[<sup>11</sup>C]LM229</b>		Increased brain uptake in P301S mice. Fast brain penetration plateaued in the first minute	McMurray et al., 2021

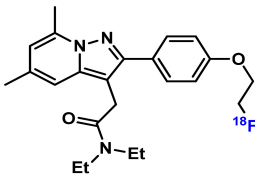
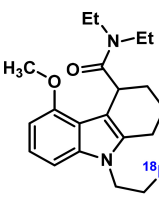
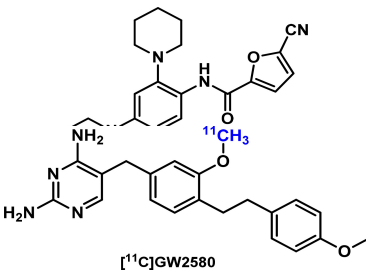
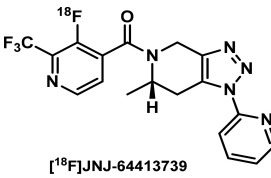
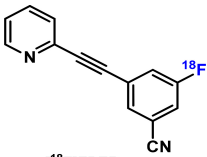
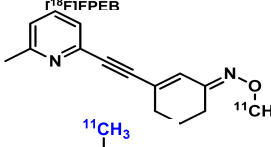
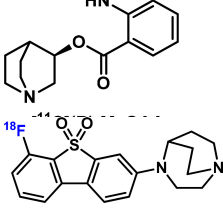
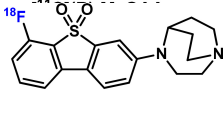
(Continued)

TABLE 4 | (Continued)

Imaging target	Tracer structure	Imaging characteristics	Major finding	Reference
	 <p>[<sup>18</sup>F]JNJ067</p>		Second-generation Tau tracer with improved specificity. Only tested in human and healthy animals	Chotipanich et al., 2020
				Guehl et al., 2019
				Sanabria Bohórquez et al., 2019
				Wong et al., 2018
				Leuzy et al., 2019
				Baker et al., 2021
Glucose	 <p>[<sup>18</sup>F]FDG</p>	Glucose metabolism	Brain [ <sup>18</sup> F]FDG PET primarily indicates synaptic activity. Hypometabolism correlates well with severity of cognitive deficits. Contradictory results found in diverse AD mouse strains.	Chiaravalloti et al., 2018
SV2A	 <p>[<sup>11</sup>C]UCB-A</p> <p>[<sup>18</sup>F]UCB-H</p> <p>[<sup>18</sup>F]SynVesT-1</p>	Synaptic vesicle glycoprotein as a general biomarker of synaptic density	Imaging data unavailable	Cai et al., 2014
			Testing in human showed slow brain kinetics	Zheng et al., 2022
			First tested in human; low specific binding signal in human brain	Bahri et al., 2017
			High specific binding signal in non-human primates and humans. Decreased uptake in APP/PS1 mice, but no difference in tg-ArcSwe mice	Xiong et al., 2021
			Decreased uptake in APP/PS1 and dKI mice	Naganawa et al., 2021

(Continued)

TABLE 4 | (Continued)

Imaging target	Tracer structure	Imaging characteristics	Major finding	Reference
TSPO	 <p><b>[<sup>18</sup>F]DPA714</b></p>	TSPO protein mainly in the outer mitochondrial membrane	Higher [ <sup>18</sup> F]DPA714 uptake was noted in the cortex and hippocampus of 12–13 and 15–16-months-old but not younger AD mice compared with control mice	Hu et al., 2020
	 <p><b>[<sup>18</sup>F]GE-180</b></p>		May be useful for tracking TSPO/neuroinflammation in early-stage AD but not for monitoring disease progression in APP23 mice	Fan et al., 2016
CSF1R	 <p><b>[<sup>11</sup>C]GW2580</b></p>	CSF1R protein on microglia, infiltrating macrophages/ monocytes and dendritic cells in the brain	Increased uptake in the brain of AD mice with overexpression of APP <sup>swe</sup> and APP Indiana mutations	Horti et al., 2019
P2 × 7R	 <p><b>[<sup>18</sup>F]JNJ-64413739</b></p>	Purinergic P2 × 7 receptor expressed in M1 microglia	Higher sensitivity than [ <sup>11</sup> C]CPPC in APP-KI mice	Zhou X. et al., 2021
			Elevated uptake in the LPS-treated site of rat brain compared with contralateral hemisphere	Berdyeva et al., 2019
mGluR5	 <p><b>[<sup>18</sup>F]FPEB</b></p>	Seven-transmembrane G protein-coupled receptors located in excitatory synapses and in glial cells	Contradictory results found in different AD strains	Varlow et al., 2020
	 <p><b>[<sup>11</sup>C]MPEB</b></p>		Signal levels correlate with progressive brain atrophy during the aging process in rTg4510 mice	Fang et al., 2017
Cholinergic α7 nAChR	 <p><b>[<sup>18</sup>F]A85380</b></p>	Cholinergic α7 nAChR	Uptake was found increased in aged monkeys	Nakaizumi et al., 2018
	 <p><b>[<sup>18</sup>F]ASEM</b></p>		Decreased uptake was seen in aged TgF334 rats	Horti et al., 2014

and Di-scFv [<sup>124</sup>I]3D6-8D3, respectively, to detect the soluble A $\beta$  in the tg-ArcSwe (A $\beta$ PP E693G) and Swedish (A $\beta$ PP KM670/671NL) mouse models with clearly visualized A $\beta$  in the brain. The brain PET imaging shows a correlation between the PET signal and the levels of soluble A $\beta$  aggregates. An increased SUVR of 2.2–3.5 in AD mice brains was reported compared to the wild-type brains. The evaluations of other amyloid imaging tracers in AD models have been summarized nicely in a recent review (Ni, 2021).

## Tau PET Imaging

Targeting another hallmark of AD, tau neurofibrillary tangle is an extremely exciting area of PET tracer development. Tau is an axonally enriched microtubule-associated protein (MAP) that accumulates in the temporal and parietal neocortex in AD brains (Hung et al., 2016; DeTure and Dickson, 2019). Tau exists as six different isoforms, which contain either 3 or 4 microtubule-binding repeats (3R or 4R). The hyperphosphorylation and aggregation of tau with different repeats are involved in different neurodegenerative diseases, e.g., AD (3R/4R), Pick disease (3R), and progressive supranuclear palsy (4R). Postmortem histopathological studies demonstrated that NFTs are a better index of disease severity and progression than A $\beta$  for patients with AD (Shoghi-Jadid et al., 2002). Tau pathology appears earlier than the A $\beta$  plaque in human brains (Arnsten et al., 2021a). Tau-PET imaging allows the detection of tauopathy and highly predicts subsequent cognitive decline in both asymptomatic and symptomatic individuals (Leuzy et al., 2019; Wang and Edison, 2019; Beyers and Brendel, 2021).

### First-Generation Tau Radioligands

[<sup>18</sup>F]FDNDP is the first PET tracer to visualize both amyloid plaques and tau tangles in living humans (Shin et al., 2011). Kuntner et al. (2009) compared 13–15-month-old age-matched wild-type litter mates with Tg2576 mice and found no difference in regional brain kinetics and DVR values. Later, the so-called first generation tau radioligand including [<sup>18</sup>F]THK523, the first tau selective tracer (Okamura et al., 2005), and other THK family tracers ([<sup>18</sup>F]THK5105, [<sup>18</sup>F]THK5117, [<sup>18</sup>F]THK5317, and [<sup>18</sup>F]THK5351) were developed and evaluated in human and AD mouse models. Fodero-Tavoletti et al. (2011) found higher retention of [<sup>18</sup>F]THK523 in the brains of rTg4510 mice compared with their wild-type littermates or 12-month-old APP/PS1 mice. Brendel et al. (2016) investigated [<sup>18</sup>F]THK5117 in Tau-P301S mice (PS19) and bigenic GSK-3 $\beta$   $\times$  Tau-P301L (biGT) mice and found increased SUVR in the brain stem of aged P301S mice and the entorhinal/amygdaloidal areas of biGT mice. In a separate study, the same group conducted a head-to-head comparison of [<sup>18</sup>F]T807 and [<sup>18</sup>F]THK5117 in Tau-P301S (P301S) mice (Brendel et al., 2018). Significantly elevated [<sup>18</sup>F]T807 than [<sup>18</sup>F]THK5117 uptake in the brainstem of P301S mice was evident at 6 months, and this increased further at 9 months. Thus, [<sup>18</sup>F]T807 appeared to be more sensitive than [<sup>18</sup>F]THK5117 to detect tau pathology in this model. Recently, [<sup>18</sup>F]THK5351 PET signal was found to correlate well with histological and biochemical tau changes, as well as motor,

memory, and learning impairment, in P301S tau mice from 8 months over time (Moreno-Gonzalez et al., 2021).

Nevertheless, due to the off-target binding to monoamine oxidase-B (MAO-B), the THK family tracers are deemed to have limited utility in imaging tauopathies in AD (Ng et al., 2017; Murugan et al., 2019; Bao et al., 2021).

[<sup>11</sup>C]PBB3 is a pyrimidinyl- and pyridinyl-butadienyl-benzothiazole and has been clinically used for *in vivo* detection of tauopathies in the human brain. [<sup>11</sup>C]PBB3 has been tested in the rTg4510 mouse (Ishikawa et al., 2018) and the PS19 transgenic mouse model (expressing 4R tau pathology) (Maruyama et al., 2013). Ni et al. (2018) compared [<sup>11</sup>C]PBB3 in PS19 and rTg4510 models and found increased binding *in vivo* in the neocortex and hippocampus of rTg4510 mice. In contrast, *in vitro* [<sup>11</sup>C]PBB3 binding was elevated in the brain stem but not in the hippocampus of PS19 mice. [<sup>18</sup>F]PM-PBB3, an <sup>18</sup>F-labeled derivative of [<sup>11</sup>C]PBB3, has been demonstrated to detect significant tau deposits as measured by SUVR in the rTg4510 mice as early as 6 months of age (Weng et al., 2020). Recently, McMurray et al. reported the synthesis of [<sup>11</sup>C]LM229 based on the backbone of PBB3. [<sup>11</sup>C]LM229 showed high specificity for 4R tau aggregated in the brain sections of P301S tau mice and truncated human 151–351 3R (SHR24) and 4R (SHR72) tau aggregates in tau transgenic rat brain sections. Preliminary PET studies with [<sup>11</sup>C]LM229 in both WT and transgenic P310S tau mice confirmed BBB penetration by the radiotracer with maximum brain uptake (%ID/g max; WT = 1.56, P301S = 2.38) within the first minute, followed by washout during the 90-min scan (McMurray et al., 2021).

The most widely studied first-generation tau radioligand [<sup>18</sup>F]flortaucipir ([<sup>18</sup>F] T-807 and [<sup>18</sup>F]AV-1451) did not show any different retention in the cerebrum of the P301L tau transgenic mice compared to wild-type mice (Xia et al., 2013; Declercq et al., 2016), which was attributed to the use of transgenic mice expressing structurally different tau deposits in the animals than in humans (Duyckaerts et al., 2008).

### Second-Generation Tau Radioligands

Second-generation radiotracers with improved signal-to-noise ratio, less off-target, and lower non-specific binding are now available for tau imaging research. These tracers include [<sup>18</sup>F]PI2620, [<sup>18</sup>F]MK6240, [<sup>18</sup>F]GTP1, [<sup>18</sup>F]RO-948 (RO6958948), [<sup>18</sup>F]JNJ311 (JNJ64349311), and [<sup>18</sup>F]JNJ-067 (JNJ-64326067). Preliminary studies have been carried out in humans and healthy mice with promising results regarding the binding selectivity, affinity, and stability (Bao et al., 2021). So far, these tracers have not been tested in AD animal models.

## PET Imaging of Glucose Metabolism

Brain [<sup>18</sup>F]FDG PET primarily indicates synaptic activity. [<sup>18</sup>F]FDG uptake strongly correlates at autopsy with levels of the synaptic vesicle protein synaptophysin (Rocher et al., 2003). The degree and regional extent of hypometabolism measured by [<sup>18</sup>F]FDG-PET roughly correlate with the overall severity of cognitive impairment in AD. There is a close correlation between the regional accumulation of a tau-PET tracer ([<sup>18</sup>F]AV1451) and [<sup>18</sup>F]FDG hypometabolism (Rubinski et al., 2020). Along with

amyloid imaging, [ $^{18}\text{F}$ ]FDG PET has been applied in multiple AD rodent models such as APP<sup>sw</sup>e (Tg2576), 5 × FAD, APP/PS1, 3 × Tg, Tg4-42, TASTPM mice, and McGill-R-Thy1-APP rats (Waldron et al., 2015b; Bouter et al., 2018; Bouter and Bouter, 2019). Varying [ $^{18}\text{F}$ ]FDG PET results were found in Tg2576 mice. No differences in cerebral glucose metabolism were found in Tg2576 compared to WT mice in Kunter's study (Kuntner et al., 2009), while Luo et al. (2012) found an increase in the FDG uptake in 7-month-old Tg2576, and Coleman et al. (2017) reported reduced FDG uptake in 18-month-old mice. Two separate [ $^{18}\text{F}$ ]FDG PET studies using 12-month-old APP<sup>PS1-21</sup> mice reached the same conclusion that FDG uptake was reduced in the brain (Waldron et al., 2015a; Takkinen et al., 2017). Using APP/PS1 mice, both Poinsel et al. (2012) and Li et al. (2016) showed an age-dependent increase in glucose metabolism. In addition, PS2APP mice showed increased [ $^{18}\text{F}$ ]FDG uptake at 5 and 16 month (Brendel et al., 2016) and TASTPM mice were found to have decreased FDG uptake at 9 and 14 months of age (Waldron et al., 2015a, 2017; Deleye et al., 2016). Contradictory results were reported in 5xFAD mice, with Rojas et al. (2013) reporting increased uptake of [ $^{18}\text{F}$ ]FDG in 11-month-old 5xFAD, and Macdonald et al. (2014) showing decreased uptake in 13-month-old mice. Sancheti et al. (2013) also reported decreased FDG uptake in 3xTg mice.

Clinical FDG PET imaging studies have shown promise in detecting early AD as neurodegeneration in certain brain regions (temporoparietal predominantly) is reflected by hypometabolism of FDG (Cohen and Klunk, 2014), and the hypometabolism pattern could serve as a predictive biomarker for conversion from MCI to AD dementia (Sala et al., 2020) earlier than MRI (Laforce Jr., Soucy et al., 2018). However, there has been no suitable method to distinguish the FDG signal contributed by neuronal activity and immune cell activation, and thus the FDG PET signal could theoretically be influenced by two opposing forces, i.e., hypometabolism and neuroinflammation, at certain stages of AD pathogenesis and progression. With the recent development of PET imaging methods for synapse density (see section "PET Imaging of Synaptic Vesicle Glycoprotein 2A" for SV2A PET) and neuroinflammation (see section "PET Imaging of Neuroinflammation" for PET imaging of neuroinflammation), we are at a stage where we could potentially quantitatively attribute the FDG signals to synaptic and glial activities. This is of relevance in cases of MCI patients who show a positive correlation between A $\beta$  PET and FDG PET.

## PET Imaging of Synaptic Vesicle Glycoprotein 2A

Synaptic Vesicle Glycoprotein 2A is ubiquitously expressed in the neurons of the central nervous system and is widely used as one of the synaptic density biomarkers. Loss of synapses in the hippocampus and prefrontal cortex is implicated as an early pathological event in AD before the appearance of A $\beta$  plaques and tau tangles and increasingly worsened during AD progression (Cai et al., 2019; Jackson et al., 2019).

[ $^{11}\text{C}$ ]Levetiracetam was first developed but was not pursued in further imaging study (Cai et al., 2014). Nevertheless, it

encouraged the development of SV2A ligands with much higher affinities, including [ $^{11}\text{C}$ ]UCB-A (Estrada et al., 2016), [ $^{18}\text{F}$ ]UCB-H (Warnock et al., 2014; Bahri et al., 2017; Becker et al., 2017), and [ $^{11}\text{C}$ ]/[ $^{18}\text{F}$ ]UCB-J (Cai et al., 2019; Li et al., 2019b). Among these, [ $^{11}\text{C}$ ]UCB-J exhibited high brain uptake, fast and reversible tissue binding kinetics, and high specific binding signals in both non-human primates and humans (Finnema et al., 2016; Nabulsi et al., 2016). Most recently, [ $^{18}\text{F}$ ]SynVesT-1 (also known as [ $^{18}\text{F}$ ]SDM-8 (Li et al., 2019a) and [ $^{18}\text{F}$ ]MNI-1126 (Constantinescu et al., 2019) are developed and evaluated in non-human primates and humans (Li et al., 2021; Naganawa et al., 2021). Using APP/PS1 mice, Toyonaga et al. showed decreased [ $^{11}\text{C}$ ]UCB-J uptake as compared to the WT mice, and treatment with the tyrosine kinase Fyn inhibitor saracatinib reversed this effect (Toyonaga et al., 2019). Sadasivam et al. (2019, 2021) found a lower [ $^{18}\text{F}$ ]SynVesT-1 signal in the whole brain of APP/PS1 mice, compared with wild-type mice (Figure 2B). However, in a study using [ $^{11}\text{C}$ ]UCB-J in the tg-ArcSwe model and wild-type mice, a small but non-significant difference (~5%) was found between the two groups, presumably due to large inter-animal variability (Xiong et al., 2021).

## PET Imaging of Neuroinflammation

Microglia are macrophages in the brain that play an important role in neuroinflammation in AD. PET imaging of biomarkers of microglia provides insights into the time course of AD pathology. However, the diverse phenotypes of activated microglia and their different roles over the course of the AD trajectory make it challenging to develop radiotracers specific for neuroinflammation in AD.

The 18kDa translocator protein (TSPO) has been widely studied as a biomarker for microglial activation for over 20 years. Early radiotracers had disadvantages of low brain penetrability, low binding affinity for TSPO, the short half-life of the radioisotope, and sensitivity of binding affinity to gene polymorphisms (Zhou R. et al., 2021). [ $^{18}\text{F}$ ]DPA714 is one of the more recent radiotracers developed for TSPO. [ $^{18}\text{F}$ ]DPA714 was evaluated in APP/PS1 mice at different months to determine the role of microglia in the pathogenesis of AD neuroinflammation (Hu et al., 2020). Higher [ $^{18}\text{F}$ ]DPA714 uptake was noted in the cortex and hippocampus of 12–13 and 15–16-months-old but not younger AD mice compared with control mice. Another longitudinal PET study in APP23 mice used [ $^{18}\text{F}$ ]GE180 for TSPO imaging and [ $^{11}\text{C}$ ]PIB for assessing amyloid deposition in *ex vivo* autoradiography experiments (Lopez-Picon et al., 2018). The APP23 model was chosen because of high [ $^{11}\text{C}$ ]PIB binding in the brain of model mice compared with other AD models such as APP/PS1. AD mice were imaged with [ $^{18}\text{F}$ ]GE-180 at 17, 20, and 26 months of age. The binding of [ $^{18}\text{F}$ ]GE-180 plateaued in the frontal cortex and hippocampus regions in the early stage of AD, but amyloidosis increased throughout the later stages of AD (17–26 months of age). Thus, [ $^{18}\text{F}$ ]GE-180 appeared to be useful for tracking TSPO/neuroinflammation in early-stage AD but not for monitoring disease progression.

Compared with TSPO, colony-stimulating factor 1 receptor (CSF1R) expression in the brain is predominantly localized to microglia and low in other cell types. [ $^{11}\text{C}$ ]CPPC was developed

from a potent CSF1R inhibitor with an  $IC_{50}$  of 0.8 nM (Horti et al., 2019) and evaluated in a mouse model of AD-related amyloidosis-overexpressing APP with Swedish and Indiana mutations (Melnikova et al., 2013). [ $^{11}C$ ]CPPC had about 30% higher uptake in the cortex of AD mice compared with control mice at 40 min post injection. Significantly higher uptake in the hippocampus and cerebellum was also observed in the AD mice. Additionally, increased expression of CSF1R after LPS treatment and about 50% specific binding of [ $^{11}C$ ]CPPC in LPS-treated mice were observed relative to sham controls. Autoradiography studies with [ $^3H$ ]CPPC demonstrated the lack of specificity of [ $^3H$ ]CPPC in brain tissues of LPS-treated Sprague-Dawley rats (Knight et al., 2021). In another study, the imaging performance of [ $^{11}C$ ]CPPC was compared with that of [ $^{11}C$ ]GW2580 in mouse models of acute and chronic neuroinflammation and a rhesus monkey (Zhou X. et al., 2021). In WT vs. APP-KI mice, [ $^{11}C$ ]GW2580 demonstrated higher sensitivity than [ $^{11}C$ ]CPPC, shown by a greater increase in [ $^{11}C$ ]GW2580 uptake in the neocortex, forebrain, and striatum of APP-KI mice compared with that in WT based on SUVR measurements at 60–90 min. Blocking studies in the monkey showed higher specificity for [ $^{11}C$ ]GW2580 over [ $^{11}C$ ]CPPC.

TREM2 is a relatively new biomarker for microglial activation. Bispecific antibody scaffolds that bind to transferrin to enter the brain and to TREM2 were chemically conjugated and radiolabeled with relatively longer-lived radioisotopes. One example is  $^{124}I$ -mAb1729-scFv8D3<sub>CL</sub>, which was evaluated in Arc-Swe transgenic AD mice (Meier et al., 2021). While areas under the curve (AUC) for  $^{124}I$ -mAb1729-scFv8D3<sub>CL</sub> at 24–72 h post injection were higher in caudate, cortex, thalamus, and hippocampus of AD mice compared with control mice, significant differences in SUVs were not observed for the individual imaging timepoints. However, *ex vivo* binding studies through autoradiography with the radiotracer showed significant differences between the animal models. The lack of a significant difference *in vivo* was then attributed to the increased blood residence time of  $^{124}I$ -mAb1729-scFv8D3<sub>CL</sub>. Thus, radiolabeling of smaller antibody fragments is desirable to address the slow pharmacokinetic issue.

Another new biomarker for AD is the purinergic P2X ligand-gated ion channel type 7 receptor (P2X7R), which is involved in triggering parts of the AD neurodegenerative processes. P2X7R activates microglia in acute AD models (Sanz et al., 2009) and increases the production of chemokines mediated by A $\beta$  peptide in chronic AD models (Martin et al., 2019). [ $^{18}F$ ]JNJ-64413739 was evaluated in a rat model of acute neuroinflammation. The uptake of [ $^{18}F$ ]JNJ-64413739 was found to be elevated in the LPS-treated site of the rat brain compared with the contralateral hemisphere of the brain treated with PBS (Berdyeva et al., 2019). Biomarkers for neuroinflammation, such as higher mRNA levels of P2X7R, TSPO, and Aif1, were associated with the LPS-treated site. It was acknowledged that LPS treatment as a model of neuroinflammation is considered extreme and that this novel tracer warrants evaluation in rodent models of AD and other neurodegenerative diseases. Other PET tracers for P2X7R and other biomarkers of neuroinflammation are reviewed by Zhou R. et al. (2021). So far, the development

of neuroinflammation imaging agents has been focused on targeting microglial activation, largely ignoring the other glial cell types. It would be instrumental to be able to distinguish the protective microglial activation in early AD from the later destructive phenotype to guide the proper timing of anti-inflammatory treatments.

## PET Imaging of NMDA Receptors

Glutamate is the major excitatory neurotransmitter in the brain and acts on the ionotropic glutamate receptors (iGluRs) and metabotropic glutamate receptors (mGluRs) to regulate synaptic plasticity. iGluRs comprise three subfamilies:  $\alpha$ -amino-3-hydroxy-5-methyl-4-isoxasolepropionic acid (AMPA) receptors, kainate receptors, and NMDARs (Traynelis et al., 2010). mGluRs are a family of G-protein-coupled receptors with 8 subtypes, mGluR1–8. Both iGluRs and mGluRs are found to be involved in synaptic malfunctions in AD (Avila et al., 2017; Foster et al., 2017; Wang and Reddy, 2017; Liu et al., 2019; Srivastava et al., 2020).

Several imaging tracers for glutamate receptors have been developed. So far, only the mGluR5 radiotracer [ $^{18}F$ ]FPEB has been evaluated in 5  $\times$  FAD mice (Lee et al., 2019), APP/PS1 mice (Varlow et al., 2020), and Tg-ArcSwe mice (Fang et al., 2017), with conflicting results: compared to wild-type animals, uptake of [ $^{18}F$ ]FPEB was found to be lower in 5  $\times$  FAD mice, with no difference in Tg-ArcSwe mice, and increased in APP/PS1 mice. Shimojo et al. (2020) observed that radioactivity signals derived from the other mGluR5 tracer (E)-[ $^{11}C$ ]ABP688 were unaltered relative to controls at 2 months of age in rTg4510 mice but then gradually declined with aging in parallel with progressive brain atrophy.

## PET Imaging of Cholinergic Targets

The deficit in cholinergic neurotransmission is a prominent pathophysiological feature in AD. Dramatic loss of cholinergic neurons located in the basal forebrain increased levels of  $\alpha_7$  nicotinic acetylcholine receptor ( $\alpha_7$  nAChR) (Ikonomic et al., 2009; Marutle et al., 2013) and decreased levels of M1 muscarinic acetylcholine receptor (M1 mAChR) (Yi et al., 2020) were found in the cortical regions of human AD brains (Ferreira-Vieira et al., 2016). The following PET imaging agents for cholinergic targets have been developed: 1) [ $^{11}C$ ]NS14492 (Ettrup et al., 2011), [ $^{11}C$ ](R)-MeQAA (Nishiyama et al., 2015), and [ $^{18}F$ ]ASEM (Gao et al., 2013) for  $\alpha_7$  nAChR; 2) [ $^{11}C$ ](+)-3-MPB (Yamamoto et al., 2011) and [ $^{18}F$ ]fluorobenzyl-dexetimide (Rowe et al., 2021) for mAChR; 3) [ $^{11}C$ ]LSN3172176 for M1 mAChR (Nabulsi et al., 2019); and 4) [ $^{11}C$ ]MK-6884 M4 mAChR (Tong et al., 2020). Uptake of the  $\alpha_7$  nAChR tracer [ $^{11}C$ ](R)-MeQAA was found to be increased in aged monkeys (Nishiyama et al., 2015), and lower uptake of the other  $\alpha_7$  nAChR tracer [ $^{18}F$ ]ASEM was seen in aged TgF334 rats compared with wild-type rats (Chaney et al., 2021). No difference was noted in the brain uptake of the acetylcholine esterase tracer [ $^{11}C$ ]MP4A between the APP23 and wild-type mice at 10–13 months of age (Heneka et al., 2006).

## Other PET Radiotracers for AD

Altered expression of endogenous cannabinoid receptor 2 (CB2), histaminergic receptors, sigma receptors, adenosine receptors (A1A and A2A receptors), and enzymes (BACE1, caspase 3, asparlyl cathepsin, and TrkB/C), as well as abnormalities in dopamine and serotonin neurotransmission, have been noted in AD. These provide additional targets for PET radiotracer development for AD imaging. The CB2 radiotracers [<sup>11</sup>C]A-836339 have been tested in the LPS-induced neuroinflammation mouse model and the Appsw/PS1/dE9 mouse model (Horti et al., 2010), while [<sup>18</sup>F]JHU94620 has been tested in the LPS-induced neuroinflammation mouse model, which shows high-affinity binding to CB<sub>2</sub>R and sufficient selectivity over CB<sub>1</sub>R. A few tracers targeting caspase 3 and asparlyl capthepsin have been tested in AD model mice, with the majority of the tracers mainly tested in human subjects.

There has been great interest in imaging the compromised BBB in animal models of amyloidosis and patients with AD, as there is evidence of damaged BBB at the early stages of AD in patients and animal models. PET imaging of specific transporters and receptors expressed at the BBB was recently reviewed thoroughly by Ni<sup>98</sup>.

## CONCLUSION AND OUTLOOK

Alzheimer's disease animal models have played essential roles in the development of PET radiotracers for imaging a diverse set of biological and pathological biomarkers in AD (Table 4). In turn, with well-validated PET tracers, PET imaging allows for longitudinal tracking of pathological phenotypes of AD in the same animals, boosting the statistical power in mechanistic studies of AD-related phenotypical and functional changes and facilitating the development of novel interventions through treatment effects monitoring. Currently, there is no perfect AD animal model that can fully recapitulate all features of human AD. However, with the rapid development in molecular biological technologies and our improved understanding of human AD etiology factors, we envision that the generation of more refined animal models with closer proximity to human AD pathogenesis will deepen our understanding of this devastating degenerative disease, further the development of biomarkers for preclinical diagnosis, and open new avenues for early and effective interventions.

Currently, PET radiotracers targeting A $\beta$  plaque, tau pathology, synaptic density, and neuroinflammation have been tested on several major AD models for their relatively prominent and consistent pathological phenotypes. To retrieve

## REFERENCES

Abey, A., Davies, D., Goldsbury, C., Buckland, M., Valenzuela, M., and Duncan, T. (2021). Distribution of tau hyperphosphorylation in canine dementia resembles early Alzheimer's disease and other tauopathies. *Brain Pathol.* 31, 144–162. doi: 10.1111/bpa.12893

the most approximate characteristics of the tracer in humans, the proper selection of AD models is key to the success of tracer development, as the neuropathological features vary based on different AD animal models. The selection of a proper AD model is also pivotal to the longitudinal and mechanistic studies of AD and anti-amyloid treatments (Manook et al., 2012; Snellman et al., 2013, 2017). One important point to bear in mind is that when choosing AD animals for PET imaging, correlation with behavioral measures, not just the AD pathologies, should be presented, and the time frame for imaging should also match those for the appearance of the biological phenotypes and related behavioral alterations.

The major advantage of using rat models of AD pathologies is their relatively large brain size, which reduces the partial volume effects in quantitative PET imaging analysis (Toyonaga et al., 2022). Rats are easier to handle than mice, less readily stressed by humans, and produce more robust behavioral testing results (Long and Holtzman, 2019). In addition, the APP/PS1 rats develop tau pathology in the brain, while the APP/PS1 mice with the same promoter lack tau pathology, indicating the APP/PS1 transgene in rats produces closer neuropathology to humans than in mice (Pini et al., 2016).

The translation and clinical A $\beta$ , tau, and FDG PET imaging have transformed our understanding of AD (Scheltens et al., 2021), generated new insights (Aschenbrenner et al., 2018), and opened an avenue for the early detection of AD (Frisoni et al., 2017). With the development of new PET imaging tracers, we expect to gain a deeper understanding of AD at the systemic level and hopefully discover and validate new treatment targets beyond A $\beta$  and tau.

## AUTHOR CONTRIBUTIONS

BC, ZC, YH, and BM-N contributed to the conception and design of the review. BC wrote the first draft of the manuscript. BC, BM-N, and ZC wrote sections of the manuscript. ZC, BC, and YH revised the manuscript and approved the final version. BC, EB, TT, and JT prepared the figure and table. All authors contributed to manuscript revision, read, and approved the submitted version.

## FUNDING

ZC was supported by grants from the National Institutes of Health (NIH) R01AG058773, R01AG069921, and the Archer Foundation.

Agca, C., Fritz, J. J., Walker, L. C., Levey, A. I., Chan, A. W., Lah, J. J., et al. (2008). Development of transgenic rats producing human beta-amyloid precursor protein as a model for Alzheimer's disease: transgene and endogenous APP genes are regulated tissue-specifically. *BMC Neurosci.* 9:28. doi: 10.1186/1471-2202-9-28

Allen, B., Ingram, E., Takao, M., Smith, M. J., Jakes, R., Virdee, K., et al. (2002). Abundant tau filaments and nonapoptotic neurodegeneration in transgenic

- mice expressing human P301S tau protein. *J. Neurosci.* 22, 9340–9351. doi: 10.1523/JNEUROSCI.22-21-09340.2002
- Alzghool, O. M., Rokka, J., López-Picón, F. R., Snellman, A., Helin, J. S., Okamura, N., et al. (2021). (S)-[18F]THK5117 brain uptake is associated with A $\beta$  plaques and MAO-B enzyme in a mouse model of Alzheimer's disease. *Neuropharmacology* 196:108676. doi: 10.1016/j.neuropharm.2021.108676
- Alzheimer's Association (2021). 2021 Alzheimer's disease facts and figures. *Alzheimers Dement.* 17, 327–406. doi: 10.1002/alz.12328
- Andorfer, C., Kress, Y., Espinoza, M., de Silva, R., Tucker, K. L., Barde, Y. A., et al. (2003). Hyperphosphorylation and aggregation of tau in mice expressing normal human tau isoforms. *J. Neurochem.* 86, 582–590. doi: 10.1046/j.1471-4159.2003.01879.x
- Arnsten, A. F. T., Datta, D., Del Tredici, K., and Braak, H. (2021a). Hypothesis: tau pathology is an initiating factor in sporadic Alzheimer's disease. *Alzheimers Dement.* 17, 115–124. doi: 10.1002/alz.12192
- Arnsten, A. F. T., Datta, D., and Preuss, T. M. (2021b). Studies of aging nonhuman primates illuminate the etiology of early-stage Alzheimer's-like neuropathology: an evolutionary perspective. *Am. J. Primatol.* 83:e23254. doi: 10.1002/ajp.23254
- Aschenbrenner, A. J., Gordon, B. A., Benzinger, T. L. S., Morris, J. C., and Hassenstab, J. J. (2018). Influence of tau PET, amyloid PET, and hippocampal volume on cognition in Alzheimer disease. *Neurology* 91, e859–e866. doi: 10.1212/WNL.00000000000006075
- Avila, J., Llorens-Martin, M., Pallas-Bazarra, N., Bolos, M., Perea, J. R., Rodriguez-Matellán, A., et al. (2017). Cognitive decline in neuronal aging and Alzheimer's disease: role of NMDA receptors and associated proteins. *Front. Neurosci.* 11:626. doi: 10.3389/fnins.2017.00626
- Bacskaï, B. J., Hickey, G. A., Skoch, J., Kajdasz, S. T., Wang, Y., Huang, G. F., et al. (2003). Four-dimensional multiphoton imaging of brain entry, amyloid binding, and clearance of an amyloid-beta ligand in transgenic mice. *Proc. Natl. Acad. Sci. U.S.A.* 100, 12462–12467. doi: 10.1073/pnas.2034101100
- Bahri, M. A., Plenevaux, A., Aerts, J., Bastin, C., Becker, G., Mercier, J., et al. (2017). Measuring brain synaptic vesicle protein 2A with positron emission tomography and [(18)F]UCB-H. *Alzheimers Dement.* 3, 481–486. doi: 10.1016/j.trci.2017.08.004
- Baker, S., and Gotz, J. (2016). A local insult of okadaic acid in wild-type mice induces tau phosphorylation and protein aggregation in anatomically distinct brain regions. *Acta Neuropathol. Commun.* 4:32. doi: 10.1186/s40478-016-0300-0
- Baker, S. L., Provost, K., Thomas, W., Whitman, A. J., Janabi, M., Schmidt, M. E., et al. (2021). Evaluation of [18F]-JN-64326067-AAA tau PET tracer in humans. *J. Cereb. Blood Flow Metab.* 41, 3302–3313. doi: 10.1177/0271678X211031035
- Bao, W., Xie, F., Zuo, C., Guan, Y., and Huang, Y. H. P. E. T. (2021). Neuroimaging of Alzheimer's disease: radiotracers and their utility in clinical research. *Front. Aging Neurosci.* 13:624330. doi: 10.3389/fnagi.2021.624330
- Becker, G., Warnier, C., Serrano, M. E., Bahri, M. A., Mercier, J., Lemaire, C., et al. (2017). Pharmacokinetic characterization of [(18)F]UCB-H PET radiopharmaceutical in the rat brain. *Mol. Pharm.* 14, 2719–2725. doi: 10.1021/acs.molpharmaceut.7b00235
- Beckman, D., Chakrabarty, P., Ott, S., Dao, A., Zhou, E., Janssen, W. G., et al. (2021). A novel tau-based rhesus monkey model of Alzheimer's pathogenesis. *Alzheimers Dement.* 17, 933–945. doi: 10.1002/alz.12318
- Benedikz, E., Kloskowska, E., and Winblad, B. (2009). The rat as an animal model of Alzheimer's disease. *J. Cell Mol. Med.* 13, 1034–1042.
- Berdyeva, T., Xia, C., Taylor, N., He, Y., Chen, G., Huang, C., et al. (2019). PET imaging of the P2X7 ion channel with a novel tracer. *Mol. Imaging Biol.* 21, 871–878. doi: 10.1007/s11307-018-01313-2
- Beyer, L., and Brendel, M. (2021). Imaging of tau pathology in neurodegenerative diseases: an update. *Semin. Nucl. Med.* 51, 253–263. doi: 10.1053/j.semnucmed.2020.12.004
- Biancalana, M., and Koide, S. (2010). Molecular mechanism of Thioflavin-T binding to amyloid fibrils. *Biochim. Biophys. Acta* 1804, 1405–1412. doi: 10.1016/j.bbapap.2010.04.001
- Bolmont, T., Clavaguera, F., Meyer-Luehmann, M., Herzog, M. C., Radde, R., Staufenbiel, M., et al. (2007). Induction of tau pathology by intracerebral infusion of amyloid-beta-containing brain extract and by amyloid-beta deposition in APP x Tau transgenic mice. *Am. J. Pathol.* 171, 2012–2020. doi: 10.2353/ajpath.2007.070403
- Bour, A., Grootendorst, J., Vogel, E., Kelche, C., Dodart, J. C., Bales, K., et al. (2008). Middle-aged human apoE4 targeted-replacement mice show retention deficits on a wide range of spatial memory tasks. *Behav. Brain Res.* 193, 174–182. doi: 10.1016/j.bbr.2008.05.008
- Bouter, C., and Bouter, Y. (2019). (18)F-FDG-PET in mouse models of Alzheimer's disease. *Front. Med.* 6:71. doi: 10.3389/fmed.2019.00071
- Bouter, C., Henniges, P., Franke, T. N., Irwin, C., Sahlmann, C. O., Sichler, M. E., et al. (2018). (18)F-FDG-PET detects drastic changes in brain metabolism in the Tg4-42 model of Alzheimer's disease. *Front. Aging Neurosci.* 10:425. doi: 10.3389/fnagi.2018.00425
- Braak, H., Braak, E., and Strothjohann, M. (1994). Abnormally phosphorylated tau protein related to the formation of neurofibrillary tangles and neuropil threads in the cerebral cortex of sheep and goat. *Neurosci. Lett.* 171, 1–4. doi: 10.1016/0304-3940(94)90589-4
- Brendel, M., Jaworska, A., Probst, F., Overhoff, F., Korzhova, V., Lindner, S., et al. (2016). Small-animal PET Imaging of tau pathology with 18F-THK5117 in 2 transgenic mouse models. *J. Nucl. Med.* 57, 792–798. doi: 10.2967/jnumed.115.163493
- Brendel, M., Yousefi, B. H., Blume, T., Herz, M., Focke, C., Deussing, M., et al. (2018). Comparison of (18)F-T807 and (18)F-THK5117 PET in a mouse model of tau pathology. *Front. Aging Neurosci.* 10:174. doi: 10.3389/fnagi.2018.00174
- Cai, H., Wang, Y., McCarthy, D., Wen, H., Borchelt, D. R., Price, D. L., et al. (2001). BACE1 is the major beta-secretase for generation of Abeta peptides by neurons. *Nat. Neurosci.* 4, 233–234. doi: 10.1038/85064
- Cai, H. C., Mangner, T., Muzik, O., and Chugani, H. (2014). Radiosynthesis and preliminary evaluation of 11C-levetiracetam for PET imaging of SV2A expression. *J. Nucl. Med.* 55, 1152–1155. doi: 10.1021/ml500285t
- Cai, Z., Li, S., Matuskey, D., Nabulsi, N., and Huang, Y. (2019). PET imaging of synaptic density: a new tool for investigation of neuropsychiatric diseases. *Neurosci. Lett.* 691, 44–50. doi: 10.1016/j.neulet.2018.07.038
- Chambers, J. K., Tokuda, T., Uchida, K., Ishii, R., Tatebe, H., Takahashi, E., et al. (2015). The domestic cat as a natural animal model of Alzheimer's disease. *Acta Neuropathol. Commun.* 3:78. doi: 10.1186/s40478-015-0258-3
- Chaney, A. M., Lopez-Picon, F. R., Serriere, S., Wang, R., Bochicchio, D., Webb, S. D., et al. (2021). Prodromal neuroinflammatory, cholinergic and metabolite dysfunction detected by PET and MRS in the TgF344-AD transgenic rat model of AD: a collaborative multi-modal study. *Theranostics* 11, 6644–6667. doi: 10.7150/thno.56059
- Charreau, B., Tesson, L., Soullou, J. P., Pourcel, C., and Anegon, I. (1996). Transgenesis in rats: technical aspects and models. *Transgen. Res.* 5, 223–234. doi: 10.1007/BF01972876
- Chiaravalloti, A., Castellano, A. E., Ricci, M., Barbagallo, G., Sannino, P., Ursini, F., et al. (2018). Coupled Imaging with [18F]FBB and [18F]FDG in AD subjects show a selective association between amyloid burden and cortical dysfunction in the brain. *Mol. Imaging Biol.* 20, 659–666. doi: 10.1007/s11307-018-1167-1
- Chiotis, K., Stenkrona, P., Almkvist, O., Stepanov, V., Ferreira, D., Arakawa, R., et al. (2018). Dual tracer tau PET imaging reveals different molecular targets for 11C-THK5351 and 11C-PBB3 in the Alzheimer brain. *Eur. J. Nucl. Med. Mol. Imaging* 45, 1605–1617. doi: 10.1007/s00259-018-4012-5
- Choi, D. Y., Lee, J. W., Lin, G., Lee, Y. K., Lee, Y. H., Choi, I. S., et al. (2012). Obovatol attenuates LPS-induced memory impairments in mice via inhibition of NF-kappaB signaling pathway. *Neurochem. Int.* 60, 68–77. doi: 10.1016/j.neuint.2011.11.005
- Chotipanich, C., Nivorn, M., Kunawudhi, A., Promteangtrong, C., Boonkwin, N., and Jantarato, A. (2020). Evaluation of imaging windows for Tau PET imaging using 18F-PI2620 in cognitively normal individuals, mild cognitive impairment, and Alzheimer's disease patients. *Mol. Imaging* 19:1536012120947582. doi: 10.1177/1536012120947582
- Clavaguera, F., Bolmont, T., Crowther, R. A., Abramowski, D., Frank, S., Probst, A., et al. (2009). Transmission and spreading of tauopathy in transgenic mouse brain. *Nat. Cell Biol.* 11, 909–913. doi: 10.1038/ncb1901
- Clavaguera, F., Hench, J., Lavenir, I., Schweighauser, G., Frank, S., Goedert, M., et al. (2014). Peripheral administration of tau aggregates triggers intracerebral tauopathy in transgenic mice. *Acta Neuropathol.* 127, 299–301. doi: 10.1007/s00401-013-1231-5
- Cohen, A. D., and Klunk, W. E. (2014). Early detection of Alzheimer's disease using PiB and FDG PET. *Neurobiol. Dis.* 72(Pt A), 117–122. doi: 10.1016/j.nbd.2014.05.001

- Cohen, R. M., Rezai-Zadeh, K., Weitz, T. M., Rentsendorj, A., Gate, D., Spivak, L., et al. (2013). A transgenic Alzheimer rat with plaques, tau pathology, behavioral impairment, oligomeric A $\beta$ , and frank neuronal loss. *J. Neurosci.* 33, 6245–6256. doi: 10.1523/JNEUROSCI.3672-12.2013
- Coleman, R. A., Liang, C., Patel, R., Ali, S., and Mukherjee, J. (2017). Brain and brown adipose tissue metabolism in transgenic Tg2576 mice models of Alzheimer disease assessed using (18)F-FDG PET imaging. *Mol. Imaging* 16:1536012117704557. doi: 10.1177/1536012117704557
- Condello, C., Lemmin, T., Stohr, J., Nick, M., Wu, Y., Maxwell, A. M., et al. (2018). Structural heterogeneity and intersubject variability of Abeta in familial and sporadic Alzheimer's disease. *Proc. Natl. Acad. Sci. U.S.A.* 115, E782–E791. doi: 10.1073/pnas.1714966115
- Constantinescu, C. C., Tresse, C., Zheng, M., Gouasmat, A., Carroll, V. M., Mistico, L., et al. (2019). Development and in vivo preclinical imaging of fluorine-18-labeled synaptic vesicle protein 2A (SV2A) PET tracers. *Mol. Imaging Biol.* 21, 509–518. doi: 10.1007/s11307-018-1260-5
- Das, B., and Yan, R. (2017). Role of BACE1 in Alzheimer's synaptic function. *Transl. Neurodegener.* 6:23. doi: 10.1186/s40035-017-0093-5
- Datta, D., Leslie, S. N., Wang, M., Morozov, Y. M., Yang, S., Mentone, S., et al. (2021). Age-related calcium dysregulation linked with tau pathology and impaired cognition in non-human primates. *Alzheimers Dement.* 17, 920–932. doi: 10.1002/alz.12325
- Dawson, H. N., Ferreira, A., Eyster, M. V., Ghoshal, N., Binder, L. I., and Vitek, M. P. (2001). Inhibition of neuronal maturation in primary hippocampal neurons from tau deficient mice. *J. Cell Sci.* 114(Pt 6), 1179–1187. doi: 10.1242/jcs.114.6.1179
- Declercq, L., Celen, S., Lecina, J., Ahamed, M., Tousseyn, T., Moechars, D., et al. (2016). Comparison of New Tau PET-Tracer Candidates With [18F]T808 and [18F]T807. *Mol. Imaging* 15:1536012115624920. doi: 10.1177/1536012115624920
- Deleay, S., Waldron, A. M., Richardson, J. C., Schmidt, M., Langlois, X., Stroobants, S., et al. (2016). The effects of physiological and methodological determinants on 18F-FDG mouse brain imaging exemplified in a double transgenic Alzheimer model. *Mol. Imaging* 15:1536012115624919. doi: 10.1177/1536012115624919
- Deleay, S., Waldron, A. M., Verhaeghe, J., Bittelbergs, A., Wyffels, L., Van Broeck, B., et al. (2017). Evaluation of small-animal PET outcome measures to detect disease modification induced by BACE inhibition in a transgenic mouse model of Alzheimer disease. *J. Nucl. Med.* 58, 1977–1983. doi: 10.2967/jnumed.116.187625
- DeTure, M. A., and Dickson, D. W. (2019). The neuropathological diagnosis of Alzheimer's disease. *Mol. Neurodegener.* 14:32.
- Duff, K., Knight, H., Refolo, L. M., Sanders, S., Yu, X., Picciano, M., et al. (2000). Characterization of pathology in transgenic mice over-expressing human genomic and cDNA tau transgenes. *Neurobiol. Dis.* 7, 87–98. doi: 10.1006/nbdi.1999.0279
- Dumanis, S. B., DiBattista, A. M., Miessau, M., Moussa, C. E., and Rebeck, G. W. (2013). APOE genotype affects the pre-synaptic compartment of glutamatergic nerve terminals. *J. Neurochem.* 124, 4–14. doi: 10.1111/j.1471-4159.2012.07908.x
- Duyckaerts, C., Potier, M. C., and Delatour, B. (2008). Alzheimer disease models and human neuropathology: similarities and differences. *Acta Neuropathol.* 115, 5–38. doi: 10.1007/s00401-007-0312-8
- Echeverria, V., Ducatenzeiler, A., Alhonen, L., Janne, J., Grant, S. M., Wandosell, F., et al. (2004a). Rat transgenic models with a phenotype of intracellular Abeta accumulation in hippocampus and cortex. *J. Alzheimers Dis.* 6, 209–219. doi: 10.3233/jad-2004-6301
- Echeverria, V., Ducatenzeiler, A., Dowd, E., Janne, J., Grant, S. M., Szyf, M., et al. (2004b). Altered mitogen-activated protein kinase signaling, tau hyperphosphorylation and mild spatial learning dysfunction in transgenic rats expressing the beta-amyloid peptide intracellularly in hippocampal and cortical neurons. *Neuroscience* 129, 583–592. doi: 10.1016/j.neuroscience.2004.07.036
- Ellenbroek, B., and Youn, J. (2016). Rodent models in neuroscience research: is it a rat race? *Dis. Model. Mech.* 9, 1079–1087. doi: 10.1242/dmm.026120
- Estrada, S., Lubberink, M., Thibblin, A., Spryca, M., Buchanan, T., Mestdagh, N., et al. (2016). [(11)C]UCB-A, a novel PET tracer for synaptic vesicle protein 2A. *Nucl. Med. Biol.* 43, 325–332. doi: 10.1016/j.nucmedbio.2016.03.004
- Ettrop, A., Mikkelsen, J. D., Lehel, S., Madsen, J., Nielsen, E. O., Palmer, M., et al. (2011). 11C-NS14492 as a novel PET radioligand for imaging cerebral alpha7 nicotinic acetylcholine receptors: in vivo evaluation and drug occupancy measurements. *J. Nucl. Med.* 52, 1449–1456. doi: 10.2967/jnumed.111.088815
- Fan, Z., Calsolaro, V., Atkinson, R. A., Femminella, G. D., Waldman, A., Buckley, C., et al. (2016). Flutriclaimide (18F-GE180) PET: first-in-human PET study of novel third-generation in vivo marker of human translocator protein. *J. Nucl. Med.* 57, 1753–1759. doi: 10.2967/jnumed.115.169078
- Fang, X. T., Eriksson, J., Antoni, G., Yngve, U., Cato, L., Lannfelt, L., et al. (2017). Brain mGluR5 in mice with amyloid beta pathology studied with in vivo [(11)C]ABP688 PET imaging and ex vivo immunoblotting. *Neuropharmacology* 113(Pt A), 293–300. doi: 10.1016/j.neuropharm.2016.10.009
- Fang, X. T., Hultqvist, G., Meier, S. R., Antoni, G., Sehlin, D., and Syvanen, S. (2019). High detection sensitivity with antibody-based PET radioligand for amyloid beta in brain. *Neuroimage* 184, 881–888. doi: 10.1016/j.neuroimage.2018.10.011
- Ferreira-Vieira, T. H., Guimaraes, I. M., Silva, F. R., and Ribeiro, F. M. (2016). Alzheimer's disease: targeting the cholinergic system. *Curr. Neuropharmacol.* 14, 101–115.
- Filipic, P., Zilka, N., Bugos, O., Kucerak, J., Koson, P., Novak, P., et al. (2012). First transgenic rat model developing progressive cortical neurofibrillary tangles. *Neurobiol. Aging* 33, 1448–1456. doi: 10.1016/j.neurobiolaging.2010.10.015
- Finnema, S. J., Nabulsi, N. B., Eid, T., Detyniecki, K., Lin, S. F., Chen, M. K., et al. (2016). Imaging synaptic density in the living human brain. *Sci. Transl. Med.* 8:348ra96. doi: 10.1126/scitranslmed.aaf6667
- Fiock, K. L., Smith, J. D., Crary, J. F., and Hefti, M. M. (2020). beta-amyloid and tau pathology in the aging feline brain. *J. Comp. Neurol.* 528, 108–113. doi: 10.1002/cne.24741
- Flood, D. G., Lin, Y. G., Lang, D. M., Trusko, S. P., Hirsch, J. D., Savage, M. J., et al. (2009). A transgenic rat model of Alzheimer's disease with extracellular Abeta deposition. *Neurobiol. Aging* 30, 1078–1090. doi: 10.1016/j.neurobiolaging.2007.10.006
- Fodero-Tavoletti, M. T., Brockschneider, D., Villemagne, V. L., Martin, L., Connor, A. R., Thiele, A., et al. (2012). In vitro characterization of [18F]-florbetaben, an Abeta imaging radiotracer. *Nucl. Med. Biol.* 39, 1042–1048. doi: 10.1016/j.nucmedbio.2012.03.001
- Fodero-Tavoletti, M. T., Okamura, N., Furumoto, S., Mulligan, R. S., Connor, A. R., McLean, C. A., et al. (2011). 18F-THK523: a novel in vivo tau imaging ligand for Alzheimer's disease. *Brain* 134(Pt 4), 1089–1100. doi: 10.1093/brain/awr038
- Foster, T. C., Kyritsopoulos, C., and Kumar, A. (2017). Central role for NMDA receptors in redox mediated impairment of synaptic function during aging and Alzheimer's disease. *Behav. Brain Res.* 322(Pt B), 223–232. doi: 10.1016/j.bbr.2016.05.012
- Frisoni, G. B., Boccardi, M., Barkhof, F., Blennow, K., Cappa, S., Chiotis, K., et al. (2017). Strategic roadmap for an early diagnosis of Alzheimer's disease based on biomarkers. *Lancet Neurol.* 16, 661–676. doi: 10.1016/S1474-4422(17)30159-X
- Games, D., Adams, D., Alessandrini, R., Barbour, R., Berthelette, P., Blackwell, C., et al. (1995). Alzheimer-type neuropathology in transgenic mice overexpressing V717F beta-amyloid precursor protein. *Nature* 373, 523–527. doi: 10.1038/373523a0
- Gao, Y., Kellar, K. J., Yasuda, R. P., Tran, T., Xiao, Y., Dannals, R. F., et al. (2013). Derivatives of dibenzothioephene for positron emission tomography imaging of alpha7-nicotinic acetylcholine receptors. *J. Med. Chem.* 56, 7574–7589. doi: 10.1021/jm401184f
- Götz, J., Bodea, L. G., and Goedert, M. (2018). Rodent models for Alzheimer disease. *Nat. Rev. Neurosci.* 19, 583–598. doi: 10.1038/s41583-018-0054-8
- Gotz, J., Chen, F., van Dorpe, J., and Nitsch, R. M. (2001). Formation of neurofibrillary tangles in P3011 tau transgenic mice induced by Abeta 42 fibrils. *Science* 293, 1491–1495. doi: 10.1126/science.1062097
- Gotz, J., Probst, A., Spillantini, M. G., Schafer, T., Jakes, R., Burki, K., et al. (1995). Somatodendritic localization and hyperphosphorylation of tau protein in transgenic mice expressing the longest human brain tau isoform. *EMBO J.* 14, 1304–1313. doi: 10.1002/j.1460-2075.1995.tb07116.x
- Grueninger, F., Bohrmann, B., Czech, C., Ballard, T. M., Frey, J. R., Weidensteiner, C., et al. (2010). Phosphorylation of Tau at S422 is enhanced by Abeta in TauPS2APP triple transgenic mice. *Neurobiol. Dis.* 37, 294–306. doi: 10.1016/j.nbd.2009.09.004
- Guehl, N. J., Wooten, D. W., Yokell, D. L., Moon, S. H., Dhaynaut, M., Katz, S., et al. (2019). Evaluation of pharmacokinetic modeling strategies for in-vivo

- quantification of tau with the radiotracer [18F]MK6240 in human subjects. *Eur. J. Nucl. Med. Mol. Imaging* 46, 2099–2111. doi: 10.1007/s00259-019-04419-z
- Haas, L. T., Salazar, S. V., Smith, L. M., Zhao, H. R., Cox, T. O., Herber, C. S., et al. (2017). Silent allosteric modulation of mGluR5 maintains glutamate signaling while rescuing Alzheimer's mouse phenotypes. *Cell Rep.* 20, 76–88. doi: 10.1016/j.celrep.2017.06.023
- Halliday, G. (2017). Pathology and hippocampal atrophy in Alzheimer's disease. *Lancet Neurol.* 16, 862–864. doi: 10.1016/S1474-4422(17)30343-5
- Haque, A., Banik, N. L., and Ray, S. K. (2008). New insights into the roles of endolysosomal cathepsins in the pathogenesis of Alzheimer's disease: cathepsin inhibitors as potential therapeutics. *CNS Neurol. Disord. Drug Targets* 7, 270–277. doi: 10.2174/187152708784936653
- Haque, R. U., and Levey, A. I. (2019). Alzheimer's disease: a clinical perspective and future nonhuman primate research opportunities. *Proc. Natl. Acad. Sci. U.S.A.* 116, 26224–26229. doi: 10.1073/pnas.1912954116
- Harada, A., Oguchi, K., Okabe, S., Kuno, J., Terada, S., Ohshima, T., et al. (1994). Altered microtubule organization in small-calibre axons of mice lacking tau protein. *Nature* 369, 488–491. doi: 10.1038/369488a0
- He, Z., Guo, J. L., McBride, J. D., Narasimhan, S., Kim, H., Changolkar, L., et al. (2018). Amyloid-beta plaques enhance Alzheimer's brain tau-seeded pathologies by facilitating neuritic plaque tau aggregation. *Nat. Med.* 24, 29–38. doi: 10.1038/nm.4443
- Heneka, M. T., Carson, M. J., El Khoury, J., Landreth, G. E., Brosseron, F., Feinstein, D. L., et al. (2015). Neuroinflammation in Alzheimer's disease. *Lancet Neurol.* 14, 388–405.
- Heneka, M. T., Ramanathan, M., Jacobs, A. H., Dumitrescu-Ozimek, L., Bilkei-Gorzo, A., Debeir, T., et al. (2006). Locus ceruleus degeneration promotes Alzheimer pathogenesis in amyloid precursor protein 23 transgenic mice. *J. Neurosci.* 26, 1343–1354. doi: 10.1523/JNEUROSCI.4236-05.2006
- Herreman, A., Hartmann, D., Annaert, W., Saftig, P., Craessaerts, K., Serneels, L., et al. (1999). Presenilin 2 deficiency causes a mild pulmonary phenotype and no changes in amyloid precursor protein processing but enhances the embryonic lethal phenotype of presenilin 1 deficiency. *Proc. Natl. Acad. Sci. U.S.A.* 96, 11872–11877. doi: 10.1073/pnas.96.21.11872
- Hoffe, B., and Holahan, M. R. (2019). The use of pigs as a translational model for studying neurodegenerative diseases. *Front. Physiol.* 10:3838. doi: 10.3389/fphys.2019.00838
- Horti, A. G., Gao, Y., Ravert, H. T., Finley, P., Valentine, H., Wong, D. F., et al. (2010). Synthesis and biodistribution of [11C]A-836339, a new potential radioligand for PET imaging of cannabinoid type 2 receptors (CB2). *Bioorg. Med. Chem.* 18, 5202–5207. doi: 10.1016/j.bmc.2010.05.058
- Horti, A. G., Gao, Y., Kuwabara, H., Wang, Y., Abazy, S., Yasuda, R. P., et al. (2014). 18F-ASEM, a radiolabeled antagonist for imaging the  $\alpha 7$ -nicotinic acetylcholine receptor with PET. *J. Nucl. Med.* 55, 672–677. doi: 10.2967/jnumed.113.132068
- Horti, A. G., Naik, R., Foss, C. A., Minn, I., Misheneva, V., Du, Y., et al. (2019). PET imaging of microglia by targeting macrophage colony-stimulating factor 1 receptor (CSF1R). *Proc. Natl. Acad. Sci. U.S.A.* 116, 1686–1691. doi: 10.1073/pnas.1812155116
- Hu, W., Pan, D., Wang, Y., Bao, W., Zuo, C., Guan, Y., et al. (2020). PET imaging for dynamically monitoring neuroinflammation in APP/PS1 mouse model using. *Front. Neurosci.* 14:810. doi: 10.3389/fnins.2020.00810
- Hung, A. S., Liang, Y., Chow, T. C., Tang, H. C., Wu, S. L., Wai, M. S., et al. (2016). Mutated tau, amyloid and neuroinflammation in Alzheimer disease-A brief review. *Prog. Histochem. Cytochem.* 51, 1–8. doi: 10.1016/j.proghi.2016.01.001
- Ikonomic, M. D., Wecker, L., Abrahamson, E. E., Wu, J., Counts, S. E., Ginsberg, S. D., et al. (2009). Cortical alpha7 nicotinic acetylcholine receptor and beta-amyloid levels in early Alzheimer disease. *Arch. Neurol.* 66, 646–651. doi: 10.1001/archneurol.2009.46
- Ishikawa, A., Tokunaga, M., Maeda, J., Minamihisamatsu, T., Shimojo, M., Takuwa, H., et al. (2018). In vivo visualization of tau accumulation, microglial activation, and brain atrophy in a mouse model of tauopathy rTg4510. *J. Alzheimers Dis.* 61, 1037–1052. doi: 10.3233/JAD-170509
- Jackson, J., Jambirina, E., Li, J., Marston, H., Menzies, F., Phillips, K., et al. (2019). Targeting the synapse in Alzheimer's disease. *Front. Neurosci.* 13:735. doi: 10.3389/fnins.2019.00735
- Jadhav, V. S., Lin, P. B. C., Pennington, T., Di Prisco, G. V., Jannu, A. J., Xu, G., et al. (2020). Trem2 Y38C mutation and loss of Trem2 impairs neuronal synapses in adult mice. *Mol. Neurodegener.* 15:62. doi: 10.1186/s13024-020-00409-0
- Jakobsen, J. E., Johansen, M. G., Schmidt, M., Liu, Y., Li, R., Callesen, H., et al. (2016). Expression of the Alzheimer's disease mutations AbetaP695sw and PSEN1M146I in double-transgenic gottingen minipigs. *J. Alzheimers Dis.* 53, 1617–1630. doi: 10.3233/JAD-160408
- Jankowsky, J. L., Fadale, D. J., Anderson, J., Xu, G. M., Gonzales, V., Jenkins, N. A., et al. (2004). Mutant presenilins specifically elevate the levels of the 42 residue beta-amyloid peptide in vivo: evidence for augmentation of a 42-specific gamma secretase. *Hum. Mol. Genet.* 13, 159–170. doi: 10.1093/hmg/ddh019
- Jankowsky, J. L., Slunt, H. H., Ratovitski, T., Jenkins, N. A., Copeland, N. G., and Borchelt, D. R. (2001). Co-expression of multiple transgenes in mouse CNS: a comparison of strategies. *Biomol. Eng.* 17, 157–165. doi: 10.1016/s1389-0344(01)00067-3
- Ji, Y., Gong, Y., Gan, W., Beach, T., Holtzman, D. M., and Wisniewski, T. (2003). Apolipoprotein E isoform-specific regulation of dendritic spine morphology in apolipoprotein E transgenic mice and Alzheimer's disease patients. *Neuroscience* 122, 305–315. doi: 10.1016/j.neuroscience.2003.08.007
- Kang, S. S., Kurti, A., Baker, K. E., Liu, C. C., Colonna, M., Ulrich, J. D., et al. (2018). Behavioral and transcriptomic analysis of Trem2-null mice: not all knockout mice are created equal. *Hum. Mol. Genet.* 27, 211–223. doi: 10.1093/hmg/ddx366
- Kaufman, A. C., Salazar, S. V., Haas, L. T., Yang, J., Kostylev, M. A., Jeng, A. T., et al. (2015). Fyn inhibition rescues established memory and synapse loss in Alzheimer mice. *Ann. Neurol.* 77, 953–971. doi: 10.1002/ana.24394
- Kim, J., Basak, J. M., and Holtzman, D. M. (2009). The role of apolipoprotein E in Alzheimer's disease. *Neuron* 63, 287–303.
- Kloskowska, E., Pham, T. M., Nilsson, T., Zhu, S., Oberg, J., Codita, A., et al. (2010). Cognitive impairment in the Tg6590 transgenic rat model of Alzheimer's disease. *J. Cell Mol. Med.* 14, 1816–1823. doi: 10.1111/j.1582-4934.2009.00809.x
- Klunk, W. E., Engler, H., Nordberg, A., Wang, Y., Blomqvist, G., Holt, D. P., et al. (2004). Imaging brain amyloid in Alzheimer's disease with Pittsburgh Compound-B. *Ann. Neurol.* 55, 306–319. doi: 10.1002/ana.20009
- Klunk, W. E., Lopresti, B. J., Ikonomic, M. D., Lefterov, I. M., Koldamova, R. P., Abrahamson, E. E., et al. (2005). Binding of the positron emission tomography tracer Pittsburgh compound-B reflects the amount of amyloid-beta in Alzheimer's disease brain but not in transgenic mouse brain. *J. Neurosci.* 25, 10598–10606. doi: 10.1523/JNEUROSCI.2990-05.2005
- Knight, A. C., Varlow, C., Zi, T., Liang, S. H., Josephson, L., Schmidt, K., et al. (2021). In vitro evaluation of [3 H]CPPC as a tool radioligand for CSF-1R. *ACS Chem. Neurosci.* 12, 998–1006. doi: 10.1021/acscchemneuro.0c00802
- Kotredes, K. P., Oblak, A., Pandey, R. S., Lin, P. B., Garceau, D., Williams, H., et al. (2021). Uncovering disease mechanisms in a novel mouse model expressing humanized APOEepsilon4 and Trem2\* R47H. *Front. Aging Neurosci.* 13:73524. doi: 10.3389/fnagi.2021.73524
- Koutseff, A., Mittelhaeuser, C., Essabri, K., Auwerx, J., and Meziane, H. (2014). Impact of the apolipoprotein E polymorphism, age and sex on neurogenesis in mice: pathophysiological relevance for Alzheimer's disease? *Brain Res.* 1542, 32–40. doi: 10.1016/j.brainres.2013.10.003
- Kragh, P. M., Nielsen, A. L., Li, J., Du, Y., Lin, L., Schmidt, M., et al. (2009). Hemizygous minipigs produced by random gene insertion and handmade cloning express the Alzheimer's disease-causing dominant mutation APPsw. *Transgenic Res.* 18, 545–558. doi: 10.1007/s12488-009-9245-4
- Kuntner, C., Kesner, A. L., Bauer, M., Kremslehner, R., Wanek, T., Mandler, M., et al. (2009). Limitations of small animal PET imaging with [18F]FDDNP and FDG for quantitative studies in a transgenic mouse model of Alzheimer's disease. *Mol. Imaging Biol.* 11, 236–240. doi: 10.1007/s11307-009-0198-z
- Laforce, R. Jr., Soucy, J. P., Sellami, L., Dallaire-Theroux, C., Brunet, F., Bergeron, D., et al. (2018). Molecular imaging in dementia: past, present, and future. *Alzheimers Dement.* 14, 1522–1552. doi: 10.1016/j.jalz.2018.06.2855
- Lee, M., Lee, H. J., Jeong, Y. J., Oh, S. J., Kang, K. J., Han, S. J., et al. (2019). Age dependency of mGluR5 availability in 5xFAD mice measured by PET. *Neurobiol. Aging* 84, 208–216. doi: 10.1016/j.neurobiolaging.2019.08.006
- Leon, W. C., Canneva, F., Partridge, V., Allard, S., Ferretti, M. T., DeWilde, A., et al. (2010). A novel transgenic rat model with a full Alzheimer's-like amyloid

- pathology displays pre-plaque intracellular amyloid-beta-associated cognitive impairment. *J. Alzheimers Dis.* 20, 113–126. doi: 10.3233/JAD-2010-1349
- Leslie, S. N., Kanyo, J., Datta, D., Wilson, R. S., Zeiss, C., Duque, A., et al. (2021). Simple, single-shot phosphoproteomic analysis of heat-stable tau identifies age-related changes in pS235- and pS396-tau levels in non-human primates. *Front. Aging Neurosci.* 13:767322. doi: 10.3389/fnagi.2021.767322
- Leuzy, A., Chiotis, K., Lemoine, L., Gillberg, P. G., Almkvist, O., Rodriguez-Vieitez, E., et al. (2019). Tau PET imaging in neurodegenerative tauopathies—still a challenge. *Mol. Psychiatry* 24, 1112–1134. doi: 10.1038/s41380-018-0342-8
- Lewandowski, C. T., Weng, J. M., and LaDu, M. J. (2020). Alzheimer's disease pathology in APOE transgenic mouse models: the who, what, when, where, why, and how. *Neurobiol. Dis.* 139:104811. doi: 10.1016/j.nbd.2020.104811
- Lewis, J., McGowan, E., Rockwood, J., Melrose, H., Nacharaju, P., Van Slegtenhorst, M., et al. (2000). Neurofibrillary tangles, amyotrophy and progressive motor disturbance in mice expressing mutant (P301L) tau protein. *Nat. Genet.* 25, 402–405. doi: 10.1038/78078
- Li, S., Naganawa, M., Pracitto, R., Najafzadeh, S., Holden, D., Henry, S., et al. (2021). Assessment of test-retest reproducibility of [(18)F]SynVesT-1, a novel radiotracer for PET imaging of synaptic vesicle glycoprotein 2A. *Eur. J. Nucl. Med. Mol. Imaging* 48, 1327–1338. doi: 10.1007/s00259-020-05149-3
- Li, S. Y., Cai, Z. X., Wu, X. A., Holden, D., Pracitto, R., Kapinos, M., et al. (2019a). Synthesis and in vivo evaluation of a novel PET radiotracer for imaging of synaptic vesicle glycoprotein 2A (SV2A) in nonhuman primates. *ACS Chem. Neurosci.* 10, 1544–1554. doi: 10.1021/acscchemneuro.8b00526
- Li, S. Y., Cai, Z. X., Zhang, W. J., Holden, D., Lin, S. F., Finnema, S. J., et al. (2019b). Synthesis and in vivo evaluation of [F-18]UCB-J for PET imaging of synaptic vesicle glycoprotein 2A (SV2A). *Eur. J. Nucl. Med. Mol. I* 46, 1952–1965. doi: 10.1007/s00259-019-04357-w
- Li, W., Wu, Y., Min, F., Li, Z., Huang, J., and Huang, R. (2010). A nonhuman primate model of Alzheimer's disease generated by intracranial injection of amyloid-beta42 and thiorphan. *Metab. Brain Dis.* 25, 277–284. doi: 10.1007/s11011-010-9207-9
- Li, X. Y., Men, W. W., Zhu, H., Lei, J. F., Zuo, F. X., Wang, Z. J., et al. (2016). Age- and brain region-specific changes of glucose metabolic disorder, learning, and memory dysfunction in early Alzheimer's disease assessed in APP/PS1 transgenic mice using (18)F-FDG-PET. *Int. J. Mol. Sci.* 17:1707. doi: 10.3390/ijms17101707
- Liu, J., Chang, L., Song, Y., Li, H., and Wu, Y. (2019). The role of NMDA receptors in Alzheimer's disease. *Front. Neurosci.* 13:43. doi: 10.3389/fnins.2019.00043
- Lo Sasso, G., Schlage, W. K., Boue, S., Veljkovic, E., Peitsch, M. C., and Hoeng, J. (2016). The ApoE(-/-) mouse model: a suitable model to study cardiovascular and respiratory diseases in the context of cigarette smoke exposure and harm reduction. *J. Transl. Med.* 14:146. doi: 10.1186/s12967-016-0901-1
- Long, J. M., and Holtzman, D. M. (2019). Alzheimer disease: an update on pathobiology and treatment strategies. *Cell* 179, 312–339. doi: 10.1016/j.cell.2019.09.001
- Lopez-Picon, F. R., Snellman, A., Eskola, O., Helin, S., Solin, O., Haaparanta-Solin, M., et al. (2018). Neuroinflammation appears early on PET imaging and then plateaus in a mouse model of alzheimer disease. *J. Nucl. Med.* 59, 509–515. doi: 10.2967/jnumed.117.197608
- Lopresti, B. J., Klunk, W. E., Mathis, C. A., Hoge, J. A., Ziolkowski, S. K., Lu, X., et al. (2005). Simplified quantification of Pittsburgh Compound B amyloid imaging PET studies: a comparative analysis. *J. Nucl. Med.* 46, 1959–1972.
- Luo, F., Rustay, N. R., Ebert, U., Hradil, V. P., Cole, T. B., Llano, D. A., et al. (2012). Characterization of 7- and 19-month-old Tg2576 mice using multimodal in vivo imaging: limitations as a translatable model of Alzheimer's disease. *Neurobiol. Aging* 33, 933–944. doi: 10.1016/j.neurobiolaging.2010.08.005
- Macdonald, I. R., DeBay, D. R., Reid, G. A., O'Leary, T. P., Jollymore, C. T., Mawko, G., et al. (2014). Early detection of cerebral glucose uptake changes in the 5XFAD mouse. *Curr. Alzheimer Res.* 11, 450–460. doi: 10.2174/1567205011666140505111354
- Maeda, J., Ji, B., Irie, T., Tomiyama, T., Maruyama, M., Okauchi, T., et al. (2007). Longitudinal, quantitative assessment of amyloid, neuroinflammation, and anti-amyloid treatment in a living mouse model of Alzheimer's disease enabled by positron emission tomography. *J. Neurosci.* 27, 10957–10968. doi: 10.1523/JNEUROSCI.0673-07.2007
- Maeda, S., Sahara, N., Saito, Y., Murayama, M., Yoshiike, Y., Kim, H., et al. (2007). Granular tau oligomers as intermediates of tau filaments. *Biochemistry* 46, 3856–3861. doi: 10.1021/bi0613590
- Manook, A., Yousefi, B. H., Willuweit, A., Platzer, S., Reder, S., Voss, A., et al. (2012). Small-animal PET imaging of amyloid-beta plaques with [(11)C]PiB and its multi-modal validation in an APP/PS1 mouse model of Alzheimer's disease. *PLoS One* 7:e31310. doi: 10.1371/journal.pone.0031310
- Martin, E., Amar, M., Dalle, C., Youssef, I., Boucher, C., Le Duigou, C., et al. (2019). New role of P2X7 receptor in an Alzheimer's disease mouse model. *Mol. Psychiatry* 24, 108–125. doi: 10.1038/s41380-018-0108-3
- Marutle, A., Gillberg, P. G., Bergfors, A., Yu, W., Ni, R., Nennesmo, I., et al. (2013). (3)H-deprenyl and (3)H-PIB autoradiography show different laminar distributions of astroglia and fibrillar beta-amyloid in Alzheimer brain. *J. Neuroinflamm.* 10:90. doi: 10.1186/1742-2094-10-90
- Maruyama, M., Shimada, H., Suhara, T., Shinotoh, H., Ji, B., Maeda, J., et al. (2013). Imaging of tau pathology in a tauopathy mouse model and in Alzheimer patients compared to normal controls. *Neuron* 79, 1094–1108. doi: 10.1016/j.neuron.2013.07.037
- McMurray, L., Macdonald, J. A., Ramakrishnan, N. K., Zhao, Y., Williamson, D. W., Tietz, O., et al. (2021). Synthesis and assessment of novel probes for imaging tau pathology in transgenic mouse and rat models. *ACS Chem. Neurosci.* 12, 1885–1893. doi: 10.1021/acscchemneuro.0c00790
- Meier, S. R., Sehlin, D., Hultqvist, G., and Syvänen, S. (2021). Pinpointing brain TREM2 levels in two mouse models of Alzheimer's disease. *Mol. Imaging Biol.* 23, 665–675. doi: 10.1007/s11307-021-01591-3
- Melnikova, T., Fromholt, S., Kim, H., Lee, D., Xu, G., Price, A., et al. (2013). Reversible pathologic and cognitive phenotypes in an inducible model of Alzheimer-amyloidosis. *J. Neurosci.* 33, 3765–3779. doi: 10.1523/JNEUROSCI.4251-12.2013
- More, S. V., Kumar, H., Cho, D. Y., Yun, Y. S., and Choi, D. K. (2016). Toxin-induced experimental models of learning and memory impairment. *Int. J. Mol. Sci.* 17:1447. doi: 10.3390/ijms17091447
- Moreno-Gonzalez, I., Edwards, G. A. III, Hasan, O., Gamez, N., Schulz, J. E., Fernandez-Valenzuela, J. J., et al. (2021). Longitudinal assessment of tau-associated pathology by (18)F-THK5351 PET imaging: a histological, biochemical, and behavioral study. *Diagnostics* 11:1874. doi: 10.3390/diagnostics11101874
- Morris, M., Maeda, S., Vessel, K., and Mucke, L. (2011). The many faces of tau. *Neuron* 70, 410–426. doi: 10.1016/j.neuron.2011.04.009
- Murugan, N. A., Chiotis, K., Rodriguez-Vieitez, E., Lemoine, L., Agren, H., and Nordberg, A. (2019). Cross-interaction of tau PET tracers with monoamine oxidase B: evidence from in silico modelling and in vivo imaging. *Eur. J. Nucl. Med. Mol. Imaging* 46, 1369–1382. doi: 10.1007/s00259-019-04305-8
- Nabulsi, N. B., Holden, D., Zheng, M. Q., Bois, F., Lin, S. F., Najafzadeh, S., et al. (2019). Evaluation of (11)C-LSN3172176 as a novel PET tracer for imaging M1 muscarinic acetylcholine receptors in nonhuman primates. *J. Nucl. Med.* 60, 1147–1153. doi: 10.2967/jnumed.118.222034
- Nabulsi, N. B., Mercier, J., Holden, D., Carre, S., Najafzadeh, S., Vandergeten, M. C., et al. (2016). Synthesis and preclinical evaluation of 11C-UCB-J as a PET tracer for imaging the synaptic vesicle glycoprotein 2A in the brain. *J. Nucl. Med.* 57, 777–784. doi: 10.2967/jnumed.115.168179
- Naganawa, M., Li, S., Nabulsi, N., Henry, S., Zheng, M. Q., Pracitto, R., et al. (2021). First-in-human evaluation of (18)F-SynVesT-1, a radioligand for PET imaging of synaptic vesicle glycoprotein 2A. *J. Nucl. Med.* 62, 561–567. doi: 10.2967/jnumed.120.249144
- Naj, A. C., and Schellenberg, G. D. (2017). Alzheimer's disease genetics, C. genomic variants, genes, and pathways of Alzheimer's disease: an overview. *Am. J. Med. Genet. B Neuropsychiatr. Genet.* 174, 5–26. doi: 10.1002/ajmg.b.32499
- Nakaizumi, K., Ouchi, Y., Terada, T., Yoshikawa, E., Kakimoto, A., Isobe, T., et al. (2018). In vivo depiction of  $\alpha 7$  nicotinic receptor loss for cognitive decline in Alzheimer's disease. *J. Alzheimers Dis.* 61, 1355–1365. doi: 10.3233/JAD-170591
- Neustadt, A. L., Winston, C. N., Parsanian, M., Main, B. S., Villapol, S., and Burns, M. P. (2017). Reduced cortical excitatory synapse number in APOE4 mice is associated with increased calcineurin activity. *Neuroreport* 28, 618–624. doi: 10.1097/WNR.0000000000000811

- Ng, K. P., Pascoal, T. A., Mathotaarachchi, S., Therriault, J., Kang, M. S., Shin, M., et al. (2017). Monoamine oxidase B inhibitor, selegiline, reduces (18)F-THK5351 uptake in the human brain. *Alzheimers Res. Ther.* 9:25. doi: 10.1186/s13195-017-0253-y
- Ni, R. (2021). Positron emission tomography in animal models of Alzheimer's disease amyloidosis: translational implications. *Pharmaceuticals* 14:1179. doi: 10.3390/ph14111179
- Ni, R., Ji, B., Ono, M., Sahara, N., Zhang, M. R., Aoki, I., et al. (2018). Comparative in vitro and in vivo quantifications of pathologic tau deposits and their association with neurodegeneration in tauopathy mouse models. *J. Nucl. Med.* 59, 960–966. doi: 10.2967/jnumed.117.201632
- Nishiyama, S., Ohba, H., Kanazawa, M., Kakiuchi, T., and Tsukada, H. (2015). Comparing alpha7 nicotinic acetylcholine receptor binding, amyloid-beta deposition, and mitochondria complex-I function in living brain: a PET study in aged monkeys. *Synapse* 69, 475–483. doi: 10.1002/syn.21842
- Oakley, H., Cole, S. L., Logan, S., Maus, E., Shao, P., Craft, J., et al. (2006). Intraneuronal beta-amyloid aggregates, neurodegeneration, and neuron loss in transgenic mice with five familial Alzheimer's disease mutations: potential factors in amyloid plaque formation. *J. Neurosci.* 26, 10129–10140. doi: 10.1523/JNEUROSCI.1202-06.2006
- Ojo, J. O., Mouzon, B., Greenberg, M. B., Bachmeier, C., Mullan, M., and Crawford, F. (2013). Repetitive mild traumatic brain injury augments tau pathology and glial activation in aged hTau mice. *J. Neuropathol. Exp. Neurol.* 72, 137–151. doi: 10.1097/NEN.0b013e3182814cdf
- Okamura, N., Furumoto, S., Fodero-Tavoletti, M. T., Mulligan, R. S., Harada, R., Yates, P., et al. (2014). Non-invasive assessment of Alzheimer's disease neurofibrillary pathology using 18F-THK5105 PET. *QARain* 137, 1762–1771. doi: 10.1093/brain/awu064
- Okamura, N., Suemoto, T., Furumoto, S., Suzuki, M., Shimadzu, H., Akatsu, H., et al. (2005). Quinoline and benzimidazole derivatives: candidate probes for in vivo imaging of tau pathology in Alzheimer's disease. *J. Neurosci.* 25, 10857–10862. doi: 10.1523/JNEUROSCI.1738-05.2005
- Ordóñez-Gutiérrez, L., Fernandez-Perez, I., Herrera, J. L., Anton, M., Benito-Cuesta, I., and Wandosell, F. (2016). AbetaPP/PS1 transgenic mice show sex differences in the cerebellum associated with aging. *J. Alzheimers Dis.* 54, 645–656. doi: 10.3233/JAD-160572
- Paspalas, C. D., Carlyle, B. C., Leslie, S., Preuss, T. M., Crimins, J. L., Huttner, A. J., et al. (2018). The aged rhesus macaque manifests Braak stage III/IV Alzheimer's-like pathology. *Alzheimers Dement.* 14, 680–691. doi: 10.1016/j.jalz.2017.11.005
- Peeraer, E., Bittelbergs, A., Van Kolen, K., Stancu, I. C., Vasconcelos, B., Mahieu, M., et al. (2015). Intracerebral injection of preformed synthetic tau fibrils initiates widespread tauopathy and neuronal loss in the brains of tau transgenic mice. *Neurobiol. Dis.* 73, 83–95. doi: 10.1016/j.nbd.2014.08.032
- Piedrahita, J. A., Zhang, S. H., Hagaman, J. R., Oliver, P. M., and Maeda, N. (1992). Generation of mice carrying a mutant apolipoprotein E gene inactivated by gene targeting in embryonic stem cells. *Proc. Natl. Acad. Sci. U.S.A.* 89, 4471–4475. doi: 10.1073/pnas.89.10.4471
- Pini, L., Pievani, M., Bocchetta, M., Altomare, D., Bosco, P., Cavedo, E., et al. (2016). Brain atrophy in Alzheimer's disease and aging. *Ageing Res. Rev.* 30, 25–48. doi: 10.1016/j.arr.2016.01.002
- Poisnel, G., Herard, A. S., El Tannir El Tayara, N., Bourrin, E., Volk, A., Kober, F., et al. (2012). Increased regional cerebral glucose uptake in an APP/PS1 model of Alzheimer's disease. *Neurobiol. Aging* 33, 1995–2005. doi: 10.1016/j.neurobiolaging.2011.09.026
- Price, J. C., Klunk, W. E., Lopresti, B. J., Lu, X., Hoge, J. A., Ziolkowski, S. K., et al. (2005). Kinetic modeling of amyloid binding in humans using PET imaging and Pittsburgh compound-B. *J. Cereb. Blood Flow Metab.* 25, 1528–1547. doi: 10.1038/sj.jcbfm.9600146
- Prpar Mihevc, S., and Majdic, G. (2019). Canine cognitive dysfunction and Alzheimer's disease - two facets of the same disease? *Front. Neurosci.* 13:604. doi: 10.3389/fnins.2019.00604
- Querol-Vilaseca, M., Colom-Cadena, M., Pegueroles, J., Nuñez-Llaves, R., Luque-Cabecerans, J., Muñoz-Llahuna, L., et al. (2019). Nanoscale structure of amyloid-β plaques in Alzheimer's disease. *Sci. Rep.* 9:5181.
- Rabinovici, G. D., Furst, A. J., O'Neil, J. P., Racine, C. A., Mormino, E. C., Baker, S. L., et al. (2007). 11C-PIB PET imaging in Alzheimer disease and frontotemporal lobar degeneration. *Neurology* 68, 1205–1212. doi: 10.1212/01.wnl.0000259035.98480.ed
- Rocher, A. B., Chapon, F., Blaizot, X., Baron, J. C., and Chavoix, C. (2003). Resting-state brain glucose utilization as measured by PET is directly related to regional synaptophysin levels: a study in baboons. *Neuroimage* 20, 1894–1898. doi: 10.1016/j.neuroimage.2003.07.002
- Rodriguez-Vieitez, E., Leuzy, A., Chiotis, K., Saint-Aubert, L., Wall, A., and Nordberg, A. (2017). Comparability of [18F]THK5317 and [11C]PIB blood flow proxy images with [18F]FDG positron emission tomography in Alzheimer's disease. *J. Cereb. Blood Flow Metab.* 37, 740–749. doi: 10.1177/0271678X16645593
- Rohn, T. T. (2010). The role of caspases in Alzheimer's disease; potential novel therapeutic opportunities. *Apoptosis* 15, 1403–1409. doi: 10.1007/s10495-010-0463-2
- Rojas, S., Herance, J. R., Gispert, J. D., Abad, S., Torrent, E., Jimenez, X., et al. (2013). In vivo evaluation of amyloid deposition and brain glucose metabolism of 5XFAD mice using positron emission tomography. *Neurobiol. Aging* 34, 1790–1798. doi: 10.1016/j.neurobiolaging.2012.12.027
- Rowe, C. C., Krishnadas, N., Ackermann, U., Dore, V., Goh, R. Y. W., Guzman, R., et al. (2021). Imaging of brain muscarinic receptors with (18)F-Fluorobenzyl-Dexetimide: a first in human study. *Psychiatry Res. Neuroimaging* 316, 111354. doi: 10.1016/j.psychres.2021.111354
- Rubinski, A., Franzmeier, N., Neitzel, J., and Ewers, M. (2020). Alzheimer's Disease Neuroimaging. I. FDG-PET hypermetabolism is associated with higher tau-PET in mild cognitive impairment at low amyloid-PET levels. *Alzheimers Res. Ther.* 12:133. doi: 10.1186/s13195-020-00702-6
- Ruiz-Opazo, N., Kosik, K. S., Lopez, L. V., Bagamasbad, P., Ponce, L. R., and Herrera, V. L. (2004). Attenuated hippocampus-dependent learning and memory decline in transgenic TgAPPsw Fischer-344 rats. *Mol. Med.* 10, 36–44. doi: 10.2119/2003-00044.herrera
- Ryan, N. S., and Rossor, M. N. (2010). Correlating familial Alzheimer's disease gene mutations with clinical phenotype. *Biomark Med.* 4, 99–112. doi: 10.2217/bmm.09.92
- Sadasivam, P., Fang, X. T., Toyonaga, T., Lee, S., Xu, Y., Zheng, M. Q., et al. (2021). Quantification of SV2A Binding in Rodent Brain Using [(18)F]SynVesT-1 and PET Imaging. *Mol. Imaging Biol.* 23, 372–381. doi: 10.1007/s11307-020-01567-9
- Sadasivam, P., Smith, L., Spurrier, J., Lee, S., Lindemann, M., Toyonaga, T., et al. (2019). The new PET tracer F-18-SDM-8 effectively detects reduced SV2a binding in a rodent model of Alzheimer's disease. *J. Cerebr. Blood F Met.* 39, 97–97.
- Saito, T., Mihira, N., Matsuba, Y., Sasaguri, H., Hashimoto, S., Narasimhan, S., et al. (2019). Humanization of the entire murine Mapt gene provides a murine model of pathological human tau propagation. *J. Biol. Chem.* 294, 12754–12765. doi: 10.1074/jbc.RA119.009487
- Sala, A., Caprioglio, C., Santangelo, R., Vanoli, E. G., Iannaccone, S., Magnani, G., et al. (2020). Brain metabolic signatures across the Alzheimer's disease spectrum. *Eur. J. Nucl. Med. Mol. Imaging* 47, 256–269. doi: 10.1007/s00259-019-04559-2
- Sanabria Bohórquez, S. S., Maorik, J., Ogasawara, A., Tinianow, J., Gill, H. S., Barret, O., et al. (2019). [18F]GTP1 (Genentech Tau Probe 1), a radioligand for detecting neurofibrillary tangle tau pathology in Alzheimer's disease. *Eur. J. Nucl. Med. Mol. Imaging* 46, 2077–2089. doi: 10.1007/s00259-019-04399-0
- Sancheti, H., Akopian, G., Yin, F., Brinton, R. D., Walsh, J. P., and Cadenas, E. (2013). Age-dependent modulation of synaptic plasticity and insulin mimetic effect of lipoic acid on a mouse model of Alzheimer's disease. *PLoS One* 8:e69830. doi: 10.1371/journal.pone.0069830
- Santacruz, K., Lewis, J., Spire, T., Paulson, J., Kotilinek, L., Ingelsson, M., et al. (2005). Tau suppression in a neurodegenerative mouse model improves memory function. *Science* 309, 476–481. doi: 10.1126/science.1113694
- Sanz, J. M., Chiozzi, P., Ferrari, D., Colaianna, M., Idzko, M., Falzoni, S., et al. (2009). Activation of microglia by amyloid {beta} requires P2X7 receptor expression. *J. Immunol.* 182, 4378–4385. doi: 10.4049/jimmunol.0803612
- Scheltens, P., De Strooper, B., Kivipelto, M., Holstege, H., Chételat, G., Teunissen, C. E., et al. (2021). Alzheimer's disease. *Lancet* 397, 1577–1590.
- Schmidt, F., Boltze, J., Jager, C., Hofmann, S., Willems, N., Seeger, J., et al. (2015). Detection and quantification of beta-amyloid, pyroglutamate, and tau in

- aged canines. *J. Neuropathol. Exp. Neurol.* 74, 912–923. doi: 10.1097/NEN.0000000000000230
- Sehlin, D., Fang, X. T., Cato, L., Antoni, G., Lannfelt, L., and Syvanen, S. (2016). Antibody-based PET imaging of amyloid beta in mouse models of Alzheimer's disease. *Nat. Commun.* 7:10759. doi: 10.1038/ncomms10759
- Senechal, Y., Kelly, P. H., and Dev, K. K. (2008). Amyloid precursor protein knockout mice show age-dependent deficits in passive avoidance learning. *Behav. Brain Res.* 186, 126–132. doi: 10.1016/j.bbr.2007.08.003
- Shaw, K. N., Commins, S., and O'Mara, S. M. (2001). Lipopolysaccharide causes deficits in spatial learning in the watermaze but not in BDNF expression in the rat dentate gyrus. *Behav. Brain Res.* 124, 47–54. doi: 10.1016/s0166-4328(01)00232-7
- Shen, J., Bronson, R. T., Chen, D. F., Xia, W., Selkoe, D. J., and Tonegawa, S. (1997). Skeletal and CNS defects in Presenilin-1-deficient mice. *Cell* 89, 629–639. doi: 10.1016/s0092-8674(00)80244-5
- Shimojo, M., Takuwa, H., Takado, Y., Tokunaga, M., Tsukamoto, S., Minatohara, K., et al. (2020). Selective disruption of inhibitory synapses leading to neuronal hyperexcitability at an early stage of tau pathogenesis in a mouse model. *J. Neurosci.* 40, 3491–3501. doi: 10.1523/JNEUROSCI.2880-19.2020
- Shin, J., Kepe, V., Barrio, J. R., and Small, G. W. (2011). The merits of FDDNP-PET imaging in Alzheimer's disease. *J. Alzheimers Dis.* 26(Suppl. 3), 135–145. doi: 10.3233/JAD-2011-0008
- Shoghi-Jadid, K., Small, G. W., Agdeppa, E. D., Kepe, V., Ercoli, L. M., Siddarth, P., et al. (2002). Localization of neurofibrillary tangles and beta-amyloid plaques in the brains of living patients with Alzheimer disease. *Am. J. Geriatr. Psychiatry* 10, 24–35. doi: 10.1097/00019442-200201000-00004
- Smolek, T., Madari, A., Farbakova, J., Kandrac, O., Jadhav, S., Cente, M., et al. (2016). Tau hyperphosphorylation in synaptosomes and neuroinflammation are associated with canine cognitive impairment. *J. Comp. Neurol.* 524, 874–895. doi: 10.1002/cne.23877
- Snellman, A., Lopez-Picon, F. R., Rokka, J., Salmona, M., Forloni, G., Scheinin, M., et al. (2013). Longitudinal amyloid imaging in mouse brain with 11C-PIB: comparison of APP23, Tg2576, and APPsw-PS1dE9 mouse models of Alzheimer disease. *J. Nucl. Med.* 54, 1434–1441. doi: 10.2967/jnumed.112.110163
- Snellman, A., Rokka, J., Lopez-Picon, F. R., Helin, S., Re, F., Loyttyniemi, E., et al. (2017). Applicability of [(11C)PIB] micro-PET imaging for in vivo follow-up of anti-amyloid treatment effects in APP23 mouse model. *Neurobiol. Aging* 57, 84–94. doi: 10.1016/j.neurobiolaging.2017.05.008
- Srivastava, A., Das, B., Yao, A. N. Y., and Yan, R. Q. (2020). Metabotropic glutamate receptors in Alzheimer's disease synaptic dysfunction: therapeutic opportunities and hope for the future. *J. Alzheimers Dis.* 78, 1345–1361. doi: 10.3233/JAD-201146
- Sturchler-Pierrat, C., Abramowski, D., Duke, M., Wiederhold, K. H., Mistl, C., Rothacher, S., et al. (1997). Two amyloid precursor protein transgenic mouse models with Alzheimer disease-like pathology. *Proc. Natl. Acad. Sci. U.S.A.* 94, 13287–13292. doi: 10.1073/pnas.94.24.13287
- Su, Y., Fu, J., Yu, J., Zhao, Q., Guan, Y., Zuo, C., et al. (2020). Tau PET imaging with [18F]PM-PBB3 in frontotemporal dementia with MAPT mutation. *J. Alzheimers Dis.* 76, 149–157. doi: 10.3233/JAD-200287
- Sun, G. Z., He, Y. C., Ma, X. K., Li, S. T., Chen, D. J., Gao, M., et al. (2017). Hippocampal synaptic and neural network deficits in young mice carrying the human APOE4 gene. *CNS Neurosci. Ther.* 23, 748–758. doi: 10.1111/cns.12720
- Tai, L. M., Youmans, K. L., Jungbauer, L., Yu, C., and Ladu, M. J. (2011). Introducing human APOE into abeta transgenic mouse models. *Int. J. Alzheimers Dis.* 2011:810981. doi: 10.4061/2011/810981
- Takkinen, J. S., Lopez-Picon, F. R., Al Majidi, R., Eskola, O., Krzyczmonik, A., Keller, T., et al. (2017). Brain energy metabolism and neuroinflammation in ageing APP/PS1-21 mice using longitudinal (18F)F-FDG and (18F)F-DPA-714 PET imaging. *J. Cereb. Blood Flow Metab.* 37, 2870–2882. doi: 10.1177/0271678X16677990
- Tauber, C., Beaufils, E., Hommet, C., Ribeiro, M., Vercouillie, J., Vierron, E., et al. (2013). QARain [18F]FDDNP binding and glucose metabolism in advanced elderly healthy subjects and Alzheimer's disease patients. *J. Alzheimers Dis.* 36, 311–320. doi: 10.3233/JAD-122068
- Tong, L., Li, W., Lo, M. M., Gao, X., Wai, J. M., Rudd, M., et al. (2020). Discovery of [(11C)MK-6884: a positron emission tomography (PET) imaging agent for the study of M4Muscarinic receptor positive allosteric modulators (PAMs) in neurodegenerative diseases. *J. Med. Chem.* 63, 2411–2425. doi: 10.1021/acs.jmedchem.9b01406
- Toyama, H., Ye, D., Ichise, M., Liow, J. S., Cai, L., Jacobowitz, D., et al. (2005). PET imaging of brain with the beta-amyloid probe, [11C]6-OH-BTA-1, in a transgenic mouse model of Alzheimer's disease. *Eur. J. Nucl. Med. Mol. Imaging* 32, 593–600. doi: 10.1007/s00259-005-1780-5
- Toyonaga, T., Fesharaki-Zadeh, A., Strittmatter, S. M., Carson, R. E., and Cai, Z. (2022). PET imaging of synaptic density: challenges and opportunities of synaptic vesicle glycoprotein 2A PET in small animal imaging. *Front. Neurosci.* 16:787404. doi: 10.3389/fnins.2022.787404
- Toyonaga, T., Smith, L. M., Finnema, S. J., Gallezot, J. D., Naganawa, M., Bini, J., et al. (2019). In vivo synaptic density imaging with (11)C-UCB-J detects treatment effects of saracatinib in a mouse model of Alzheimer disease. *J. Nucl. Med.* 60, 1780–1786. doi: 10.2967/jnumed.118.223867
- Tran, H. T., LaFerla, F. M., Holtzman, D. M., and Brody, D. L. (2011). Controlled cortical impact traumatic brain injury in 3xTg-AD mice causes acute intra-axonal amyloid-beta accumulation and independently accelerates the development of tau abnormalities. *J. Neurosci.* 31, 9513–9525. doi: 10.1523/JNEUROSCI.0858-11.2011
- Traynelis, S. F., Wollmuth, L. P., McBain, C. J., Menniti, F. S., Vance, K. M., Ogden, K. K., et al. (2010). Glutamate receptor ion channels: structure, regulation, and function. *Pharmacol. Rev.* 62, 405–496. doi: 10.1124/pr.109.002451
- Tucker, K. L., Meyer, M., and Barde, Y. A. (2001). Neurotrophins are required for nerve growth during development. *Nat. Neurosci.* 4, 29–37. doi: 10.1038/82868
- Varlow, C., Murrell, E., Holland, J. P., Kassenbrock, A., Shannon, W., Liang, S. H., et al. (2020). Revisiting the radiosynthesis of [(18F)F]PEB and preliminary PET imaging in a mouse model of Alzheimer's disease. *Molecules* 25:982. doi: 10.3390/molecules25040982
- Waldron, A. M., Verhaeghe, J., Wyffels, L., Schmidt, M., Langlois, X., Van Der Linden, A., et al. (2015a). Preclinical comparison of the amyloid-beta radioligands [(11C)Pittsburgh compound B and [(18F)F]florbetaben in aged APPPS1-21 and BRI1-42 mouse models of cerebral amyloidosis. *Mol. Imaging Biol.* 17, 688–696. doi: 10.1007/s11307-015-0833-9
- Waldron, A. M., Wintmolders, C., Bittelbergs, A., Kelley, J. B., Schmidt, M. E., Stroobants, S., et al. (2015b). In vivo molecular neuroimaging of glucose utilization and its association with fibrillar amyloid-beta load in aged APPPS1-21 mice. *Alzheimers Res. Ther.* 7:76. doi: 10.1186/s13195-015-0158-6
- Waldron, A. M., Wyffels, L., Verhaeghe, J., Richardson, J. C., Schmidt, M., Stroobants, S., et al. (2017). Longitudinal characterization of [18F]-FDG and [18F]-AV45 uptake in the double transgenic TASTPM mouse model. *J. Alzheimers Dis.* 55, 1537–1548. doi: 10.3233/JAD-160760
- Wang, C., Wilson, W. A., Moore, S. D., Mace, B. E., Maeda, N., Schmechel, D. E., et al. (2005). Human apoE4-targeted replacement mice display synaptic deficits in the absence of neuropathology. *Neurobiol. Dis.* 18, 390–398. doi: 10.1016/j.nbd.2004.10.013
- Wang, H. F., Tan, L., Cao, L., Zhu, X. C., Jiang, T., Tan, M. S., et al. (2016). Alzheimer's disease neuroimaging, I. Application of the IWG-2 diagnostic criteria for Alzheimer's disease to the ADNI. *J. Alzheimers Dis.* 51, 227–236. doi: 10.3233/JAD-150824
- Wang, R., and Reddy, P. H. (2017). Role of glutamate and NMDA receptors in Alzheimer's disease. *J. Alzheimers Dis.* 57, 1041–1048. doi: 10.3233/JAD-160763
- Wang, Y. T., and Edison, P. (2019). Tau imaging in neurodegenerative diseases using positron emission tomography. *Curr. Neurol. Neurosci. Rep.* 19:45. doi: 10.1007/s11910-019-0962-7
- Warnock, G. I., Aerts, J., Bahri, M. A., Bretin, F., Lemaire, C., Giacomelli, F., et al. (2014). Evaluation of 18F-UCB-H as a novel PET tracer for synaptic vesicle protein 2A in the brain. *J. Nucl. Med.* 55, 1336–1341. doi: 10.2967/jnumed.113.136143
- Weng, C. C., Hsiao, I. T., Yang, Q. F., Yao, C. H., Tai, C. Y., Wu, M. F., et al. (2020). Characterization of (18F)F-PM-PBB3 ((18F)F-APN-1607) uptake in the rTg4510 mouse model of tauopathy. *Molecules* 25:1750. doi: 10.3390/molecules25071750
- Wolfe, C. M., Fitz, N. F., Nam, K. N., Lefterov, I., and Koldamova, R. (2018). The role of APOE and TREM2 in Alzheimer's disease-current understanding and perspectives. *Int. J. Mol. Sci.* 20:81. doi: 10.3390/ijms20010081
- Wong, D. F., Comley, R. A., Kuwabara, H., Rosenberg, P. B., Resnick, S. M., Ostrowitzki, S., et al. (2018). Characterization of 3 novel tau radiopharmaceuticals, 11C-RO-963, 11C-RO-643, and 18F-RO-948, in healthy

- controls and in alzheimer subjects. *J. Nucl. Med.* 59, 1869–1876. doi: 10.2967/jnumed.118.209916
- Xia, C. F., Arteaga, J., Chen, G., Gangadharmath, U., Gomez, L. F., Kasi, D., et al. (2013). [(18F)T807, a novel tau positron emission tomography imaging agent for Alzheimer's disease. *Alzheimers Dement.* 9, 666–676. doi: 10.1016/j.jalz.2012.11.008
- Xiang, X., Piers, T. M., Wefers, B., Zhu, K., Mallach, A., Brunner, B., et al. (2018). The Trem2 R47H Alzheimer's risk variant impairs splicing and reduces Trem2 mRNA and protein in mice but not in humans. *Mol. Neurodegener.* 13:49. doi: 10.1186/s13024-018-0280-6
- Xiong, M., Roshanbin, S., Rokka, J., Schlein, E., Ingelsson, M., Sehlin, D., et al. (2021). In vivo imaging of synaptic density with [(11)C]UCB-J PET in two mouse models of neurodegenerative disease. *Neuroimage* 239:118302. doi: 10.1016/j.neuroimage.2021.118302
- Xu, G., Ran, Y., Fromholt, S. E., Fu, C., Yachnis, A. T., Golde, T. E., et al. (2015). Murine Abeta over-production produces diffuse and compact Alzheimer-type amyloid deposits. *Acta Neuropathol. Commun.* 3:72. doi: 10.1186/s40478-015-0252-9
- Yaghmoor, F., Noorsaeed, A., Alsaggaf, S., Aljohani, W., Scholtzova, H., Boutajangout, A., et al. (2014). The role of TREM2 in Alzheimer's disease and other neurological disorders. *J. Alzheimers Dis. Parkinson.* 4:160. doi: 10.4172/2161-0460.1000160
- Yamamoto, S., Nishiyama, S., Kawamata, M., Ohba, H., Wakuda, T., Takei, N., et al. (2011). Muscarinic receptor occupancy and cognitive impairment: a PET study with [(11)C](+)-3-MPB and scopolamine in conscious monkeys. *Neuropsychopharmacology* 36, 1455–1465. doi: 10.1038/npp.2011.31
- Yi, J. H., Whitcomb, D. J., Park, S. J., Martinez-Perez, C., Barbati, S. A., Mitchell, S. J., et al. (2020). M1 muscarinic acetylcholine receptor dysfunction in moderate Alzheimer's disease pathology. *Brain Commun.* 2:fcaa058. doi: 10.1093/braincomms/fcaa058
- Yu, C. H., Song, G. S., Yhee, J. Y., Kim, J. H., Im, K. S., Nho, W. G., et al. (2011). Histopathological and immunohistochemical comparison of the brain of human patients with Alzheimer's disease and the brain of aged dogs with cognitive dysfunction. *J. Comp. Pathol.* 145, 45–58. doi: 10.1016/j.jcpa.2010.11.004
- Yu, F., Zhang, Y., and Chuang, D. M. (2012). Lithium reduces BACE1 overexpression, beta amyloid accumulation, and spatial learning deficits in mice with traumatic brain injury. *J. Neurotrauma* 29, 2342–2351. doi: 10.1089/neu.2012.2449
- Zeydan, B., Schwarz, C. G., Przybelski, S. A., Lesnick, T. G., Kremers, W. K., Senjem, M. L., et al. (2021). Comparison of 11 C-Pittsburgh compound-B and 18 F-flutemetamol white matter binding in PET. *J. Nucl. Med.* doi: 10.2967/jnumed.121.263281 [Epub ahead of print].
- Zhao, J., Bi, W., Xiao, S., Lan, X., Cheng, X., Zhang, J., et al. (2019). Neuroinflammation induced by lipopolysaccharide causes cognitive impairment in mice. *Sci. Rep.* 9:5790. doi: 10.1038/s41598-019-42286-8
- Zheng, C., Holden, D., Zheng, M. Q., Pracitto, R., Wilcox, K. C., Lindemann, M., et al. (2022). A metabolically stable PET tracer for imaging synaptic vesicle protein 2A: synthesis and preclinical characterization of [18F]SDM-16. *Eur. J. Nucl. Med. Mol. Imaging* 49, 1482–1496. doi: 10.1007/s00259-021-05597-5
- Zhou, R., Ji, B., Kong, Y., Qin, L., Ren, W., Guan, Y., et al. (2021). PET imaging of neuroinflammation in Alzheimer's disease. *Front. Immunol.* 12:739130. doi: 10.3389/fimmu.2021.739130
- Zhou, X., Ji, B., Seki, C., Nagai, Y., Minamimoto, T., Fujinaga, M., et al. (2021). PET imaging of colony-stimulating factor 1 receptor: a head-to-head comparison of a novel radioligand. *J. Cereb. Blood Flow Metab.* 41, 2410–2422. doi: 10.1177/0271678X211004146
- Zhu, Y., Nwabuisi-Heath, E., Dumanis, S. B., Tai, L. M., Yu, C., Rebeck, G. W., et al. (2012). APOE genotype alters glial activation and loss of synaptic markers in mice. *Glia* 60, 559–569. doi: 10.1002/glia.22289

**Author Disclaimer:** The contents are solely the responsibility of the authors and do not necessarily represent the official view of the funding agencies.

**Conflict of Interest:** The authors declare that the research was conducted in the absence of any commercial or financial relationships that could be construed as a potential conflict of interest.

**Publisher's Note:** All claims expressed in this article are solely those of the authors and do not necessarily represent those of their affiliated organizations, or those of the publisher, the editors and the reviewers. Any product that may be evaluated in this article, or claim that may be made by its manufacturer, is not guaranteed or endorsed by the publisher.

Copyright © 2022 Chen, Marquez-Nostra, Belitzky, Toyonaga, Tong, Huang and Cai. This is an open-access article distributed under the terms of the Creative Commons Attribution License (CC BY). The use, distribution or reproduction in other forums is permitted, provided the original author(s) and the copyright owner(s) are credited and that the original publication in this journal is cited, in accordance with accepted academic practice. No use, distribution or reproduction is permitted which does not comply with these terms.